## Metal-Based Soft Materials for Various Applications

M.Sc. Research Thesis

By

#### **RITIK**



# DEPARTMENT OF CHEMISTRY INDIAN INSTITUTE OF TECHNOLOGY INDORE MAY, 2023

## Metal-Based Soft Materials for Various Applications

#### **A THESIS**

Submitted in fulfillment of the requirements for the award of the degree

of

**Master of Science** 

By

**RITIK** 



## DEPARTMENT OF CHEMISTRY INDIAN INSTITUTE OF TECHNOLOGY INDORE

**MAY, 2023** 





#### INDIAN INSTITUTE OF TECHNOLOGY **INDORE**

#### CANDIDATE'S DECLARATION

I hereby certify that the work which is being presented in the thesis entitled "Metal Based Soft Materials in Various Applications" in the partial fulfilment of the requirements for the award of the degree of MASTER OF SCIENCE and submitted in the DEPARTMENT OF CHEMISTRY, INDIAN INSTITUTE OF TECHNOLOGY INDORE, is an authentic record of my own work carried out during the time period from July 2022 to May 2023 under the supervision of Dr. Suman Mukhopadhyay, Professor, IIT Indore.

The matter presented in this thesis has not been submitted by me for the award of any other degree at this or any other institute.

Ritik

This is to confirm that the candidate's above statement is true to the best of my/ our knowledge.

Prof. Suman Mukhopadhyay

Ritik has successfully given his M.Sc. Oral Examination held on 16/05/2023

E 19/05/2023 Signature of Supervisor of M.Sc. Thesis

Prof. Suman Mukhopadhyay

Date:

5.50-19/08/2023 Convener, DPGC

Dr. Umesh A. Kshirsagar (Dr. Selvakum)
Date:

Acting Drac

Signature of PSPC Member 1

Prof. Sampak Samanta

Date: 19 105 2023

Signature of PSPC Member 2

Dr. Selvakumar Sermadurai

Date: 19/00/2022

#### **ACKNOWLEDGMENTS**

I want to take this occasion to express my appreciation to everyone who helped me to finish my project report from the verse viewpoints. I want to thank everyone who contributed to this project for being crucial to my work.

First and foremost, I would like to express my sincere gratitude and respect to my supervisor, Prof. Suman Mukhopadhyay, for his constant guidance and support during this project. I feel fortunate to have had the chance to learn from him and gain a positive attitude toward life. I owe him tremendous gratitude for his unceasing support in academics and emotional well-being.

The PSPC members Prof. Sampak Samanta and Dr. Selvakumar Sermadurai, as well as DPGC convener Dr. Umesh A. Kahirsagar, have my deepest thanks for their sincere recommendations and motivation.

I also like to thank our esteemed director, Prof. Suhas Joshi, and the head of the chemistry department, Prof. Tushar Kanti Mukherjee, for providing the necessary resources and a favorable research environment. I would also like to thank the chemistry department's professors for their encouragement and continuous inspiration.

I thank my mentor, Mr. Sayantan Sarkar, for his assistance and priceless commitment to this project. These few months have been made memorable by his gentle and kind nature. He has always given me unwavering support whenever I've been in a tough spot. His suggestions and assistance helped me complete this project. I'm also thankful for the service I received from the other lab members during my project.

I also like to thank Mr. Ghanshyam Bhavsar, Mr. Kinny Pandey and Chemistry Office for their crucial help and quick technical support, without which I would not have been able to continue working on my research project.

I want to express my gratitude to my parents, Miss Veena, and my sisters, Miss Sakshi Rani and Miss Pooja Rani, for their undying support and affection. My mother and sisters have always supported me, been there for me no matter what, and always motivated me to keep going. I'm grateful for them. I also want to thank my family members, who have always supported me and given me advice when I've failed. They deserve special consideration for the unwavering love they have always shown me.

#### **RITIK**

Department of chemistry, IIT Indore

# TO...... MY MOTHER, ELDER SISTERS AND ALL WELL-WISHERS



#### **ABSTRACT**

Gelator 5,5',5"-((1,3,5-triazine-2,4,6-triyl)tris(azanediyl)) molecule triisophthalic acid (A2) is synthesized to fabricate organogel and Cu metallogel in DMSO:water mixture in 1:2 proportions. The fabricated gels have shown heat and pH-responsive behavior. Among these two fabricated gels the organogel shows thixotropic behavior. The synthesized organogel and Cu metallogel showed efficient iodine adsorption in the pores of the gel matrices. To the best of our knowledge, this is the first study where iodine adsorption takes place in the gel state. The iodine adsorption capacity from the hexane solution of iodine was found to be 2.5 mgmg<sup>-1</sup> and 1.7 mgmg<sup>-1</sup> for organogel and Cu metallogel respectively. Owing to the non-cytotoxicity and biocompatibility of the A2 gelator molecule it was further utilized to fabricate a new gel Ru@A2 using a ruthenium-based metal complex with anticancer properties. The complex incorporated gel Ru@A2 was used as a delivery vehicle to deliver the anticancer complex. The IC<sub>50</sub> value for the loaded drug was nearly 9.69 µM on HeLa cancer cells indicating intriguing cytotoxicity. The targeted drug delivery to cancer cells has been achieved using A2 as the delivery agent.



#### **TABLE OF CONTENTS**

LIS	T OF FIGURES	xiii-xiv
LIS	T OF TABLES	XV
LIS	T OF SCHEMES	XV
NO	MENCLATURE	xvi
AC	RONYMS	xvii
Ch	apter 1: Introduction	1-8
1.1	Basic Introduction	1-2
1.2	Classification of Gels	2-4
1.3	Metallogels: Properties and Characterization	4-5
1.4	Radioactive Iodine	6-7
1.5	Drug Delivery	7
1.6	Organization of Thesis	8
Cha	pter 2: Literature Survey and Project Motivation	9-12
2.1	Review of Past Work and Project Motivation	9-12
Cha	pter 3: Experimental Section	13-18
3.1	Reagents and Chemicals	13
3.2	Methods and Instrumentation	13
3.3	Synthesis of Gelator, Metallogel and Organogel	14-15
	3.3.1 Synthesis of gelator molecule <b>A2</b>	14
	3.3.2 Organogel formation from <b>A2</b>	14
	3.3.3 Metallogel formation from <b>A2</b>	14
	3.3.4 Melting temperature of gels	15
	3.3.5 Synthesis of drug C1	15
3.4	Iodine Adsorption Study in Hexane	15-16
3.5	Vapour Phase Iodine Adsorption	16-17
3.6	Drug Loading	17
3.7	Drug Release Study	17
3.8	Cytotoxicity Study	17-18

Cha	pter 4: Results and Discussions	19-41
4.1	Synthesis and Characterization	19
4.2	Reaction Scheme	19
4.3	NMR Spectra	20
4.4	Solubility of A2 and Gelation Behavior	22-23
4.5	Rheological Data	24-26
4.6	FESEM Analysis	26-27
4.7	Thermogravimetric Analysis	28
4.8	XPS Spectra	28-29
4.9	BET Data	29-30
4.10	Iodine Adsorption in Vapour Phase	30-31
4.11	Iodine Adsorption by Organogel and Cu Metallogel	31-35
4.12	Targeted Drug Delivery	35-41
	4.12.1 Drug Loading	36-37
	4.12.2 Drug Release	37-39
	4.12.3 MTT Assay	40-41
Chaj	pter 5: Conclusion and Future Scope	43-44
Refe	rences	45-50

#### LIST OF FIGURES

Figure No.	Description	Page No.
Figure 1.1	Modes of aggregation	2
Figure 1.2	Classification of gels on the basis of gel component	3
Figure 1.3	Classification of gels on the basis of gel occurrence	3
Figure 1.4	Environmental hazards of radioactive iodine	6
Figure 2.1	Molecular structures of gelators leading to	9
8	gelation	
Figure 4.1a	<sup>1</sup> H NMR spectrum of <b>A2</b>	20
Figure 4.1b	<sup>13</sup> C NMR spectrum of <b>A2</b>	20
Figure 4.2	<sup>1</sup> H NMR spectrum of <b>C1</b>	21
Figure 4.3	Inversion test of organogel of <b>A2</b> and Cu metallogel	23
Figure 4.4	a) Linear viscoelastic behaviour for <b>A2</b> organogel	24
Figure 4.5	<ul><li>(b) Dynamic frequency sweep for the A2 organogel</li><li>a) Linear viscoelastic behaviour for Cu</li></ul>	25
	b) Dynamic frequency sweep for the Cu	25
Figure 4.6	metallogel Time oscilation sweep experiment of organogel <b>A2</b>	25
Figure 4.7	(a) Linear viscoelastic behaviour for <b>Ru@A2</b> metallogel (b) Dynamic frequency sweep for the <b>Ru@A2</b> metallogel	26
Figure 4.8	FE-SEM images of organogel A2	26
Figure 4.9	FE-SEM images of Cu metallogel	26
Figure 4.10	Elemental mapping of organogel A2	27
Figure 4.11	Elemental mapping of Cu metallogel	27
Figure 4.12	EDX analysis of organogel <b>A2</b>	27
Figure 4.13	EDX analysis of Cu metallogel	27
Figure 4.14	TGA analysis of organogel <b>A2</b> , and Cu metallogel	28
Figure 4.15	XPS surface spectra (a)Nitrogen survey of OG (b) Cu survey of Cu metallogel (c) Surface spectra of OG (d) Surface spectra of Cu metallogel	
Figure 4.16	N <sub>2</sub> adsorption and desorption profile of (a) organogel and (b) Cu metallogel at 77K	29
Figure 4.17	BJH pore size distribution for (a) organogel (b) Cu metallogel	30
Figure 4.18	Adsorption of vapour iodine by organogel and Cu metallogel	30

Figure 4.19	(a) TGA analysis of I <sub>2</sub> @OG and I <sub>2</sub> @Cu (b) XPS	31
E: 4.20	spectra of I <sub>2</sub> @Cu (c) XPS spectra of I <sub>2</sub> @OG	2.1
Figure 4.20	FESEM images of (a) I <sub>2</sub> @OG and (b) I <sub>2</sub> @Cu	31
Figure 4.21	(a) Time dependent iodine adsorption by	32
	organogel (b) % removal of iodine with time (c)	
F: 4.22	concentration of iodine left (time dependent)	22
Figure 4.22	(a) Time dependent iodine adsorption by Cu	32
	metallogel (b) % removal of iodine with time (c)	
E: 4.22	concentration of iodine left (time dependent)	22
Figure 4.23	(a) Kinetics of iodine adsorption by organogel (b)	32
Eigene 4.24	Kinetics of iodine adsorption by Cu metallogel	33
Figure 4.24	Non-linear Langmuir adsorption isotherm for organogel	33
Figure 4.25	Non-linear Langmuir adsorption isotherm for	33
Figure 4.25	Cu metallogel	33
Figure 4.26	(a) UV-vis of iodine release from organogel (b)	33
riguit 4.20	(a) UV-vis of iodine release from Cu metallogel	33
	(c)Reusability of organogel for iodine capture (d)	
	Reusability of Cu metallogel for iodine capture	
Figure 4.27	(a) Comparison of IR spectra of Cu metallogel	34
rigure 1.27	and iodine adsorbed Cu metallogel (b)	٥.
	Comparison of IR spectra of organogel and	
	iodine adsorbed organogel	
Figure 4.28	(a) N1s XPS spectra of OG (b) N1s XPS spectra	35
8	of I <sub>2</sub> @OG (c) N1s XPS spectra of Cu metallogel	
	(d) N1s XPS spectra of I <sub>2</sub> @Cu	
Figure 4.29	(a) UV-vis spectra of Ru@A2 (b) IR spectra of	36
S	Ru@A2	
Figure 4.30	a) PXRD spectra of <b>Ru</b> @ <b>A2</b> (b) TGA analysis	37
8	of Ru@A2	
Figure 4.31	FESEM image of Ru@A2	37
Figure 4.32	(a) ESI-MS spectrum of liquid residue after	38
S	drug release (b) ESI-MS spectrum of solid	
	residue after drug release	
Figure 4.33	<sup>1</sup> H NMR spectra of liquid residue after drug	38
	release	
Figure 4.34	<sup>1</sup> H NMR spectra of solid residue after drug	39
	release	
Figure 4.35	Drug release profile of <b>Ru@A2</b>	39
Figure 4.36	MTT Assay of A2 organogel and Ru@A2 gel	40
_	on HeLa cells	
Figure 4.37	MTT Assay of A2 organogel and Ru@A2 gel	41
	on HEK 293 cells	

#### LIST OF TABLES

Table No. Description	Page	No.
Table 4.1 Solubility of gelator molecule in various solvents		22
Table 4.2 Optimization table for gelation with gelator		23
Table 4.3 Optimization table for gelation with solvent volum	ne	23
<b>Table 4.4</b> IC <sub>50</sub> values for cytotoxicity of drug on HeLa cance	r cells	40
<b>Table 4.5</b> IC <sub>50</sub> values for cytotoxicity on HEK 293 cancer cel	ls	41

#### LIST OF SCHEMES

Scheme No.	Description	Page No.
Scheme 4.1	Synthesis of A2	19
Scheme 4.1	Synthesis of C1	19
Scheme 4.3	Ru-based anticancer drug loading on A2 gel	36

#### NOMENCLATURE

 $\theta$  Angle

Å Angstrom

**cm** Centimetre

δ Chemical shift (N.M.R.)

°C Degree Centigrade

υ Frequency

**g** Gram

**mg** Milligram

μL Micro Litre

**mM** Milli Molar

**mmol** Milli Mole

mL Milli Litre

M Molar

**mol** Mole

**nm** Nanometer

% Percentage

s Seconds

**Λ** Wavelength

#### ACRONYMS

**AIEE** Aggregation induced emission enhancement

C Carbon

Cu Copper

**Cd** Cadmium

**DMSO** Dimethyl sulphoxide

**DMF** Dimethyl formamide

**ESI-MS** Electrospray Ionization-Mass Spectrometry

**FE-SEM** Field Emission Scanning Electron Microscope

**FT-IR** Fourier Transform-Infrared

H Hydrogen

LMWG Low Molecular Weight Gelator

MeOH Methanol

N Nitrogen

NMR Nuclear Magnetic Resonance

O Oxygen

**PXRD** Powder X-Ray Diffraction

H<sub>2</sub>O Water

**XPS** X-Ray photoelectron spectroscopy



#### **CHAPTER 1**

#### **Introduction**

#### 1.1 Basic Introduction

Gels are supramolecular assembly of gelators, formed with immobilized solvents assisted by noncovalent interactions in-between the gelator and solvent molecules such as  $\pi$ - $\pi$  stacking, hydrogen bonds, van der Waals forces, halogen bonds, hydrophobic and electrostatic interactions, etc. Several solvents like DMF, DMSO, CCl<sub>4</sub>, methanol, ethanol, THF, DCM, ACN, etc. 1-3, get immobilized into bonding sites of the gelator molecules yielding a gel. Gels have intriguing applications in various fields like drug delivery, molecular recognition, chiral recognition, electronic and optoelectronic devices, biochemistry, biomineralization, tissue engineering, catalysts, magnetic devices, lithography, dye adsorption, etc. 4-12 Several low molecular weight gelators, such as urea derivatives, sugars, modified peptides, amides, saccharides, etc., can yield gels but designing a gelator is still a massive task as it is not possible to completely rationalize the design of gelator molecules. However, it has been found that gel materials can be fabricated with a significant variation of structural units as unlimited unions of inorganic and organic units are available. 13 Organic gelator molecules can lead to the formation of organogels, where assimilation of metal ions in the gelator to form metallogel opens up the possibilities to explore various other applications in different domains. In some reported cases, the addition of metals leads to gelation due to metal-ligand interactions.<sup>14</sup>

Soft gel materials can show reversible stimuli-responsive behavior on applying heat, pressure, pH change etc.<sup>6,15</sup> Gels are also known to show UV response in some instances, as keeping the gel in UV light leads to the fabrication/breaking of gel.<sup>16</sup> Aggregation of the gelator molecules by simple heating or cooling can lead to three probable results, *viz.* crystallization, gelation, and precipitation.<sup>17</sup>

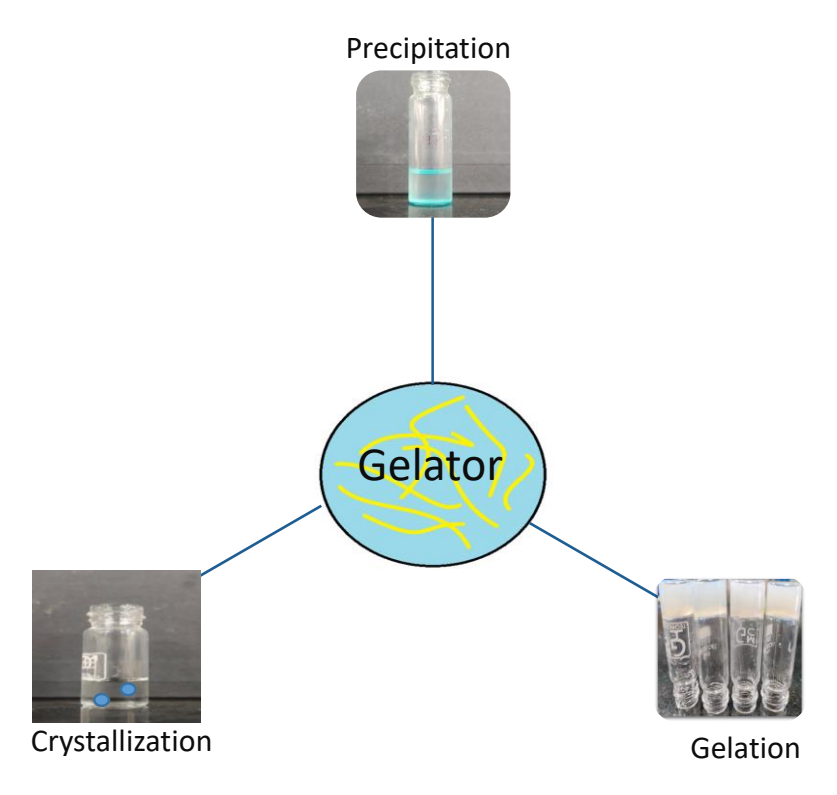


Figure 1.1: Modes of aggregation

#### 1.2 Classification of Gels

Gels can be classified in different ways based on various aspects. Based on the components present in the gel, two types of classifications are possible: gels containing metals, and gel containing no metals. Gels which contain metal ion/complex are known as metallogels. Further, these metallogels can be divided into two sub-categories: (i) gel with metal complex, in which the gelator molecule itself is the metal complex. These metal complexes assembled through various non-covalent interactions which leads to the fabrication of gels. In this case the complex itself is responsible for inducing gelation, (ii) coordination polymer gel, in which there is direct linkage of metal ions with gelator molecule and the metal-ligand interaction is the key to gelation.<sup>1-3</sup>

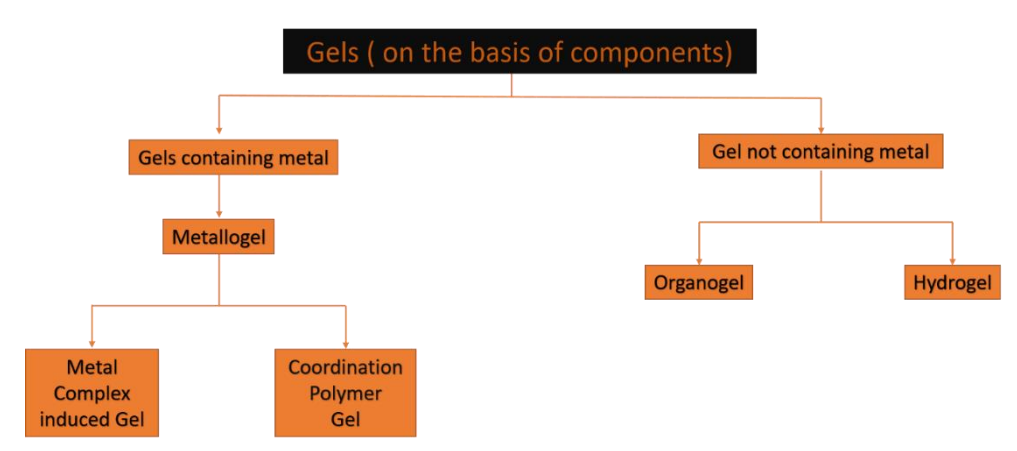


Figure 1.2: Classification of gels on the basis of gel component

Gels containing no metal ion/complex can further be subdivided into two groups on the basis of solvent entrapped in the gelator cavities: (i) organogels, in which the organic solvents are trapped, (ii) hydrogels, in which water molecules are trapped.

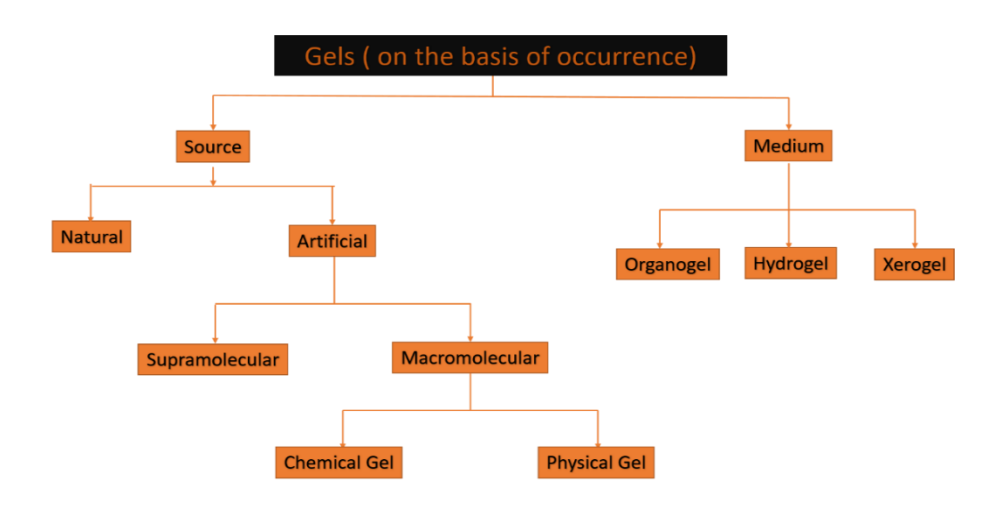


Figure 1.3: Classification of gels on the basis of gel occurrence

Further, on the basis of occurrence, gels can be classified into two categories: source and medium. Based on source, gels can be again classified into natural gels (gelatin, alginate, chitosan) and artificial gels (man-made). Further artificial gels on the basis of the constitution can be subdivided into supramolecular and macromolecular gels. Supramolecular gels are formed due to the presence of weak, reversible noncovalent interactions between low molecular weight gelators

(LMWG), whereas macromolecular gels are formed due to the presence of strong covalent bonds between the crosslinking gelators.

Further, these crosslinking macromolecular polymers can be divided into two categories: (i) chemical gel formed due to covalent bonds, which are non-reversible in nature, (ii) physical gel formed due to weak noncovalent interactions between the gelator molecule which can cause gel to sol phase transition.<sup>18</sup>

#### 1.3 Metallogels: Properties and Characterization

Fabrication of gels can get materialized by dissolving the gelator molecules and entrapping solvents in its pores. This entrapping of solvent into the gelator leads to the formation of elongated fibrils, which forms a 3D network assembly known as gel. As reported, in some cases instant gel formation occurs but in some cases, gelation is initiated only due to stimuli-response such as change in pH<sup>19</sup>, sonochemical behavior<sup>16</sup>, heat response<sup>16</sup>, etc.

The gel fabrication can be analyzed at varying concentrations of LMWG. The minimal concentration of gelator needed to build a gel network that can enclose a particular solvent is known as the critical gel concentration (CGC).<sup>20</sup>

The mechanical strength of the gel is a significant characteristic which can be analyzed using rheology. It is the study of measurement of flow and deformation of gel by applying stress/strain on the material. In rheological tests, the gel is treated to oscillatory stress, and the material's response is assessed in terms of its elastic (storage modulus- G') and viscous (loss modulus-G") properties. This method allows for the distinction between soft gels and hard gels. For hard gels G'>>G" is observed at all frequencies, whereas in soft gels, G'>G" is observed only at high frequencies and G'<G" is observed at low frequencies. Rheology is also used to calculate the gel point which is defined as the point at which G' begins to exceed G". This study also helps to determine the thixotropic behavior (self-healing) of gels by time oscillation sweep

experiment. It is a critical characteristic property of gel where the gel self-heals and regenerates after application of external stimuli (pressure).<sup>21</sup>

Fourier transform infrared spectroscopy, or FTIR is a useful tool for determining the functional groups present in the gelator and the interactions occurring with these functional groups. These interactions are responsible for the formation of a 3D gelator network leading to gel formation and they are evident from the changes in intensity and shifts in the IR band.

The <sup>1</sup>H NMR spectrum can also provide information about the gelator network's stability. In this purpose gel formation is done using deuterated solvents, and <sup>1</sup>H NMR spectra is measured at various temperatures, including those below and above the melting point of the gel (T<sub>gel</sub>). Any signal recorded belongs to the gelator molecule that is either aggregated or disaggregated in the immobilized solvent. As the temperature rises, so does the number of dissolved gelator molecules. As a result, the signal intensity increases. Temperature can also cause an up or downfield shift in the signals.

The morphology of gels can be elucidated by various microscopic techniques up to the scale of nanometers. FESEM (Scanning Electron Microscopy) and TEM (transmission electron microscopy) are the methods used for the elucidation of morphologies of gel. For the study of noncovalent interactions present in the gel, PXRD (powder X-ray diffraction), FTIR, and NMR studies are done.

In some cases, the formation of gels can lead to AIEE (aggregation-induced enhanced emission), leading to an increase in emission intensity, or ACQ (aggregation-induced quenching), leading to a decrease in emission intensity.<sup>22–24</sup>

#### 1.4 Radioactive Iodine

The use of uranium atoms in atomic bombs and nuclear fission of U-235 in nuclear reactors leads to the production of various byproducts. Out of those, <sup>129</sup>I and <sup>131</sup>I are major byproducts which are radioactive and highly volatile. The half-life of <sup>129</sup>I and <sup>131</sup>I is 15.6 million years and eight days, respectively. <sup>25</sup> When inhaled by humans in the gaseous state, radioactive iodine reaches the blood stream. It ultimately accumulates in the thyroid gland, disrupting the normal metabolic system and causing various diseases like thyroid cancer. <sup>26</sup>

Radioactive iodine can also exist in particulate form or as solution in water. Thus, it can contaminate the drinking water, soil, and cause harm to plants. For example, the iodine accumulated on the grasses on which cattle feed reaches the human metabolic system upon consuming dairy products and causes various diseases and adverse effects on the metabolic system.

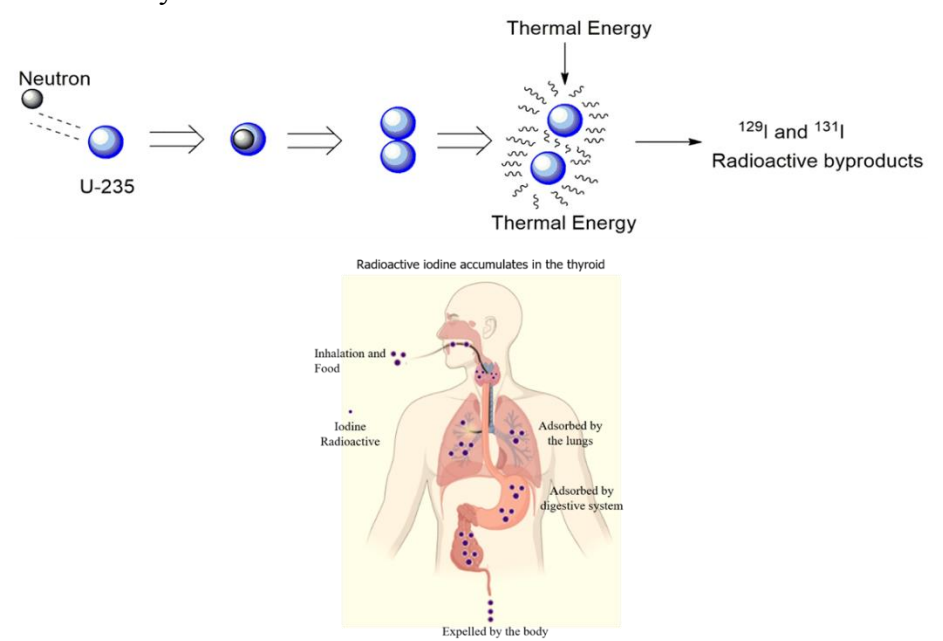


Figure 1.4: Environmental hazards of radioactive iodine

Various materials are conventionally used in iodine adsorption, such as zeolites, silver-clay materials, COFs, MOFs, etc. But these materials come with multiple disadvantages, such as high cost, non-reversibility, low efficiency, etc. Among the various emerging adsorbents, gels have emerged as a promising material due to its easy and inexpensive

synthesis strategy, easy pore tuning facility, large surface area and recyclability.<sup>27</sup> Considering these unique features, gels could be a potential candidate for efficient iodine adsorption.

#### 1.5 Drug Delivery

Drug delivery involves release of drug molecules in a controlled manner at the specific targeted site for which the drug is designed. The release of drugs from the matrix of the gel network is of great interest as gels are known to show pH-responsive behavior.<sup>28</sup>

In the drug delivery system, a host is used as the drug carrier to deliver the loaded drug to the targeted sites. The conventional drug delivery approach in which drugs are delivered to the body directly using injections, pills or solutions suffers some problems such as use of high doses of drug to avoid degradation before reaching the target, dilution of the drug in the body and poor transportation of hydrophobic drugs. The high drug doses can have several side effects such as weakening of the immune system, vomiting, headache etc.<sup>29</sup>

To decrease the demerits of conventional drug delivery approach, discovering new ways of drug delivery has become the current area of interest in the scientific community. The most efficient one out of those is gel matrix. Drugs can be loaded in the cavities of the gel by noncovalent interactions, which can be released in the body by applying external stimuli.

The advantages of using gel for drug delivery are as follows: (i) the drug can be administrated to the targeted site without getting degraded before reaching the targeted site. (ii) even low drug doses are capable of providing local drug concentration at the targeted site. (3) drug delivery will be slower by the material, leading to an increased period of time for drug release, thereby increasing the treatment time. Thus, utilizing supramolecular gels instead of the conventional drug delivery approach is advantageous in various aspects of life.<sup>30</sup>

#### 1.6 Organization of the Thesis

The aim of this project is the synthesis of a LMWG molecule **A2**, fabrication of organogel and metallogels using the synthesized gelator and to investigate the various properties of the fabricated gels for various prospected applications.

**Chapter 2** This chapter discusses the literature survey, previous work done in the area of organogels and metallogels, and motivation for the project's work.

**Chapter 3** The experimental procedure for fabrication of gels and the instruments used have been discussed in this chapter.

**Chapter 4** This chapter consists of results and discussion obtained from the synthesis of organogel and metallogels and their application in iodine adsorption and drug delivery.

**Chapter 5** The summary of the project and the future plan is provided in this thesis chapter.

#### **CHAPTER 2**

#### **Literature Survey and Project Motivation**

#### 2.1 Review of Past Work and Project Motivation

Several reports on the fabrication of supramolecular gels by the self-assembly of low molecular weight gelator molecules are there that utilizes several non-covalent interactions like H-bonding, hydrophobic interactions, pi-pi stacking, and intercolumnar stacking. Solvents that entrap in the gels play a vital role in gel formation as it facilitates H-bonding interaction. Such H-bonding interactions are generally facilitates in the presence of amide and carboxylic acid functional groups.

Figure 2.1: Molecular structures of gelators leading to gelation<sup>31–37</sup>

The molecules shown in figure 2.1 have been reported to show gelation due to presence of non-covalent interactions. The amide and carboxylic group enhanced the H-bonding interaction as evident from the change in the IR spectra. High  $\pi$  electron density present in the gelator due to

aromatic rings lead to  $\pi$ - $\pi$  interaction and intercolumnar stacking. The decrease in various gelation facilitating functionalities also affects the mechanical strength of gel. **1** (figure 2.1) forms a strong gel with a storage modulus of 27254 Pa.<sup>31</sup> Whereas molecule **7** (figure 2.1) leads to formation of a weaker gel with storage modulus of 586 Pa, and for **8** (figure 2.1) the storage modulus decreases to 236 Pa.<sup>32,33</sup> It is noteworthy to mention that most of the above mentioned gelator molecules possess C<sub>3</sub> symmetry.<sup>34–37</sup>

Gels have applications in various fields such as catalysis, environmental remediation, drug delivery, electronic devices etc. For the mitigation of environmental hazards, removal of highly volatile and radioactive iodine is of utmost interest. There are several reports where covalent organic frameworks (COF) and metal organic frameworks (MOF) have been used for iodine capture. A triazine based COF was reported by Nu and coworkers to capture iodine in vapour phase with an adsorption capacity of 6110 mgg<sup>-1</sup> of COF. Weak molecular interactions of I<sub>3</sub> with triazine unit and imine bond were responsible for iodine adsorption<sup>38</sup> But these materials have some demerits such as low stability, nonreusability, expensive and difficult to synthesize. Owing to the several interactions present inside the gel matrix these materials could be a suitable alternative of the conventionally used materials. In a latest report by Mondal et al., a Zr-based diimide gel was used to capture iodine from vapor state with an adsorption efficiency of 232 wt% of iodine.<sup>27</sup> Interaction between the C=C of the pristine ligand and iodide ion was cited as the main reason for the high iodine uptake, and this was further confirmed by the change in the FTIR spectra. The storage modulus of the gel was 106598 Pa indicating the hardness of the gel. Another strong magnesium-based metallogel with a storage modulus of more than 10<sup>5</sup> was reported for iodine sequestration with an efficacy of 587 mggm<sup>-1</sup> of gel. The high strength of the gel leads to its reusable property till four cycles.<sup>39</sup>

In a recent report by Marullo *et al.*, surfactant-based eutectogels were reported using cetyldiethanolamine-N-oxide in four eutectic mixtures.

The gel showed an iodine adsorption capacity of 280 mgg<sup>-1</sup> and a storage modulus value of 640 Pa. The gel was recyclable up to six cycles.<sup>40</sup>

At the same time due to responses to several external stimuli like pH, sonography or UV-vis irradiation, soft gels could be a suitable material for targeted and sustained drug delivery. Generally, gels with a lower or intermediate value of storage modulus is preferred for such action. Sarkar *et al.* reported a urea-based supramolecular metallogel of Zn(II) as an anticancer drug delivery agent for doxorubicin. The gel was pH sensitive and a release of 43% was observed in case of acidic pH compared to only 23% at neutral pH. The lower value of storage modulus for Zn metallogel around 1500 Pa facilitated the drug release.<sup>34</sup>

Rambabu *et al.*, reported metallogels of Cu(I) and Fe (II) using thiourea and fumaric acid based gelator molecules to deliver the anticancer drug 5-fluorouracil. The gels were pH sensitive and released a higher % of drug in acidic pH (characteristic of cancer cells) when compared to neutral pH (healthy cells).<sup>41</sup>

In a report by Lee *et al.*, a polymeric calix[4] arene-based soft gel with storage modulus of 796 Pa was reported to load and deliver a chemotherapy drug (gossypol).<sup>42</sup> In another report by Chang *et al.*, polymeric peptide based thermo sensitive hydrogels were synthesized. The gels upon increasing the temperature lead to the release of the hydrophobic anti-cancer drug paclitaxel. The low storage modulus value of around 800 Pa enhances the sustained delivery of drug.<sup>43</sup>

From the above literature survey and previous reports, it is evident that functional groups like carboxylic acid and amide groups are one of the integral part in gel fabrication strategy. Also, gels with higher value of storage modulus are favourable for usage in environmental remediation as it improves its reusability. Thus, a low molecular weight gelator molecule which is already reported to form lanthanide gel was used to form organogel and various metallogels.<sup>44</sup> The  $\pi$ -electron cloud and carboxylic acid functionality helps in gelation. The molecule was also designed to possess C<sub>3</sub> symmetry, as C<sub>3</sub> symmetric molecules are known

to have better non covalent interactions due to its orientation. As observed, soft gels or gels with intermediate values of storage modulus are favoured for drug delivery purpose. Since the main objective of the project was to investigate the application of our gel in the field of environmental remediation as well as drug delivery, the gelator was designed in such a way that it can have moderate storage modulus value.

#### **CHAPTER 3**

#### **EXPERIMENTAL SECTION**

#### 3.1 Reagents & Chemicals

Cyanuric chloride, 5-aminoisophtallic acid, copper acetate, and ruthenium chloride was purchased from Sigma-Aldrich. NaOH, NaHCO<sub>3</sub> were purchased from AVRA chemicals. Dioxane, DMSO, methanol, acetone was purchased from FINAR and used without additional purification. Copper perchlorate was synthesized in the laboratory by the reported procedure.<sup>45</sup>

#### 3.2 Instrumentation and Methods

The Perkin Elmer's spectrum II instrument was utilized to measure IR spectra in the 4000-400 cm<sup>-1</sup> range with a 4 cm<sup>-1</sup> resolution having 1s intervals. NMR spectra were obtained using AVANCE NEO500 Ascend Bruker BioSpin international AG equipment with TMS as the standard reference at room temperature. The morphology of the gels was obtained using a Supra55 Zeiss field emission scanning electron microscope (FE-SEM). The rheological experiment was done to study the organogel and metallogels strength. The rheology behavior was analyzed on a PP25 mm plate with a gap of 0.5 mm using an Anton Paar Physica MCR 301 rheometer at 25 °C. The G' and G" were measured at 0.1 percent strain to determine viscoelasticity. TGA was done using Mettler Toledo Thermal Analyzer with heating at a rate of 10 °C. Gas adsorption measurements were carried out using Quantachrome, Autosorb iQ2 Brunauer-Emmett-Teller (BET) surface area analyzer was used. PXRD of the gel was done on Empyrean, Malvern Panalytical, with Cu-Kα radiation with 2θ range from 3° to 60°. X-ray photoelectron spectroscopy (XPS) were performed through a Physical Electronics make PHI 5000 VersaProbe III (Mg K $\alpha$  X-rays, h $\nu$  = 1253.6 eV). Absorption spectra were monitored by using PerkinElmer UV/vis/NIR spectrometer in a quartz cuvette (1 cm  $\times$  1 cm).

#### 3.3 Synthesis of Gelator, Metallogel, Organogel

## 3.3.1 Synthesis of gelator molecule 5,5',5"-((1,3,5-triazine-2,4,6-triyl)tris(azanediyl))triisophthalic acid (A2)

The synthesis of gelator molecule **A2** was done by the reported procedure. In a typical reaction, 0.53 g (13.4 mmol) of NaOH and 0.87 g (10.4 mmol) of NaHCO<sub>3</sub> was added into a 25 mL round bottom flask and dissolved in 10 mL of MQ-H<sub>2</sub>O. To it 1.52 g (8.4 mmol) of 5-aminoisophtallic acid was added. Then the mixture was stirred for forty-five minutes in an ice-cold bath. After stirring, 0.37 g (2 mmol) of cyanuric chloride was dissolved in 1,4-dioxane and added dropwise into the reaction mixture. The solution was refluxed in an oil bath at 100 °C for twenty four hours. After cooling, the pH was adjusted to 2 by addition of conc. HCl. The precipitated solid was isolated by filtration, washed with MQ-H<sub>2</sub>O three times and with hot methanol three times. The solid product was dried in a vacuum desiccator.

#### 3.3.2 Organogel formation from A2 gelator

Organogel **A2** was formed in DMSO:H<sub>2</sub>O in the ratio of 0.65:0.35. 15 mg (0.024 mmol) of gelator **A2** was dissolved in 0.65 mL of DMSO, and then 0.35 mL of MQ-H<sub>2</sub>O was added slowly and homogeneously which lead to the formation of organogel **A2**. The gel formation was instant and confirmed by the test tube inversion method.

#### 3.3.3 Metallogel formation from A2 gelator

Aqueous solution of Cu salt and solution of gelator **A2** in DMSO, when mixed together leads to the formation of Cu metallogel. 15 mg (0.024 mmol) of gelator molecule **A2** was dissolved in 0.65 mL of DMSO, and the corresponding metal salts (0.0024 mmol) dissolved in 0.35 mL MQ-H<sub>2</sub>O was added slowly and homogeneously, leading to the formation of metallogels. The gel formation was instant and confirmed by the test tube inversion method.

#### 3.3.4 Melting temperature of gels (T<sub>gel</sub>)

The gel-sol transition behavior was analyzed using an oil bath. A glass vial containing the gel was immersed in an oil bath. A steel ball was placed on the gel surface, and a thermometer was used to measure the temperature. When the gel started to melt, the steel ball began to move down the gel surface; then, heating was turned off, and the temperature was noted. After several minutes, the sol turns back into the gel. The gel melting point is the sol-gel transition temperature.

#### 3.3.5 Synthesis of drug C1

C1 [Ru( $\eta^6$ -p-cym)(L)Cl] was synthesized by addition of 10 mL methanolic solution of 0.04 g of ligand (0.16 mmol) in a dropwise manner to 10 mL methanolic solution of 0.05 g [Ru(p-cymene)Cl<sub>2</sub>]<sub>2</sub> (0.08 mmol), solution was stirred at room temperature for 6 hours. The solution was reduced under pressure to obtain orange-brownish coloured compound. Yield-68%.

#### 3.4 Iodine Adsorption Study

In order to investigate the adsorption capacity of iodine in hexane by the gel matrix, 3 mL of 1 mM iodine solution in hexane was layered on 1 mL of gel (same for both organogel and metallogel) in 5 mL vials. The decrease in concentration was monitored using UV-Vis spectroscopy at a difference of 2-minute time interval. From the time dependent UV-Vis spectra the percentage adsorption of iodine and decrease in concentration of iodine was determined using the following equation:

$$D_t = \frac{C_0 - C_t}{C_0} \times 100\% = \frac{A_0 - A_t}{A_0} \times 100\%$$

where  $D_t$  is the exchange capacity,  $C_0$  and  $A_0$  are the initial concentration and absorbance of the iodine solution respectively,  $C_t$  and  $A_t$  represent the concentration and absorbance of the iodine solution at specific times respectively.

Kinetics data for adsorbed iodine was fitted in the pseudo-second-order model using the following equation:

$$Q_t = \frac{k_2 Q_e^2 t}{1 + k_2 Q_e t}$$

where t is the time in minutes, and  $Q_t$  and  $Q_e$  are the amounts of adsorbate (mgg<sup>-1</sup>) on the adsorbent at different time intervals and equilibrium respectively.

For Langmuir adsorption isotherm experiment, on 1 mL of gel, different concentration of iodine solution in hexane was layered. After 12 hours the solution was collected and the concentration was determined by UV-Vis spectroscopy. The obtained data was fitted using the following equation

$$Q_e = \frac{Q_m C_e}{K_d + C_e}$$

where,  $C_e$  (mM) and  $Q_e$  (mgg<sup>-1</sup>) are the concentration of iodine and amount of iodine adsorbed at equilibrium respectively.  $Q_m$  (mgg<sup>-1</sup>) is the maximum amount of iodine per unit mass of adsorbent to form a complete monolayer.  $K_d$  (mgmL<sup>-1</sup>) is a constant related to the affinity of the binding sites.

#### 3.5 Vapour Phase Iodine Adsorption

Iodine adsorption in vapour state was performed by placing 10 mg of xerogel of both organogel and Cu metallogel in small glass vials. The xerogel containing vials were placed in a closed container containing an excess amount of iodine granules. The whole chamber was placed in a hot plate and heated at 75° C. In the initial one hour the colour of the xerogel changes to deep brown. The heating process was continued for twelve hours and the gravimetric measurement was taken after one hour. The iodine uptake in the solid state was calculated using the following equation:

$$\alpha = \frac{m_t - m_0}{m_0} \times 100\%$$

where  $\alpha$  is the iodine uptake capacity,  $m_t$  and  $m_0$  represent the mass weight of the xerogels after and before the iodine capture.

#### 3.6 Drug Loading:

**A2** gelator molecule (0.024 mmol) was dissolved in 0.65 mL of DMSO in a 5 mL vial, followed by the addition of 0.024 mmol of **C1** [Ru( $\eta^6$ -p-cym)(L)Cl] drug molecule. The homogeneous addition of 0.35 mL of H<sub>2</sub>O in the solution leads to the formation of drug-loaded metallogel gel (**Ru@A2**).

#### 3.7 Drug Release:

Since cancer cells have an acidic environment, the release of drug was monitored at two different pH. Acidic pH of 5.6 was used to replicate the tumour cell environment and neutral pH of 7.4 was used to replicate the normal cell environment. The release of C1 from Ru@A2 gel matrix was done by layering Ru@A2 gel with PBS buffer at room temperature. 1 mL of Ru@A2 was layered with 3 mL of PBS buffer of different pH, and was allowed to stand for forty-eight hours. The amount of drug released was determined using UV-Vis spectroscopy from the absorbance of the peak at 374 nm using the following equation:

$$D_t = \frac{C_0 - C_t}{C_0} \times 100\% = \frac{A_0 - A_t}{A_0} \times 100\%$$

where  $D_t$  is the exchange capacity,  $C_0$  and  $A_0$  are the initial concentration and absorbance of C1 drug respectively, and  $C_t$  and  $A_t$  is the concentration and absorbance of C1 drug at specific times, respectively.

### 3.8 Cytotoxicity Study

Cell viability assay/ MTT assay was performed on HeLa cancer cells, by seeding a 96-well plate with HeLa cells (around 2000 cells per well). The cancer cells were incubated for twenty-four hours in  $CO_2$  atmosphere for growth and attachment. After twenty-four hours the cells were treated with varying concentrations (0.25-100  $\mu$ M) of **A2** gelator and Ru@A2 separately and left to incubate for another twenty-four

hours. This was followed by discarding the cell culture medium and adding 10  $\mu$ L of MTT solution (5 mgmL<sup>-1</sup> in PBS) per well. This was again incubated for four hours in dark. After four hours, MTT dye was discarded and DMSO was added to solubilize the purple coloured formazan product. The experiment was done in triplicates, and the cell medium without any treatment was considered as the control for the experiment. The absorbance of MTT was analysed colorimetrically at 570 nm using an ELISA microplate reader. Percentage cell viability was calculated using:

% cell viability = 
$$\frac{\text{(OD value of treated cells)}}{\text{(OD value of untreated cells (control)}} \times 100$$

IC<sub>50</sub> value, i.e., concentration of drug that kills 50% cancer cells was calculated by the absorbance (OD) versus concentration linear plot using Prism GraphPad software package.

# **CHAPTER 4**

# **Results and Discussion**

## 4.1 Synthesis and Characterization

#### 5,5',5"-((1,3,5-triazine-2,4,6-triyl)tris(azanediyl))triisophthalic acid

(A2), gelator was synthesized by the previously reported method. Gel formation due to self-assembly was observed on adding DMSO:H<sub>2</sub>O solvent in a proportion of 2:1. The rheology study was done to check the stability and strength of the gel. Various characterization was done for the same gelator molecule.

## **4.2 Reaction Scheme:**

#### 4.2.1 Synthesis of gelator A2:

Scheme 4.1: Synthesis of A2

#### 4.2.2 Synthesis of complex C1:

Scheme 4.2: Synthesis of C1

# 4.3 NMR Spectra:

NMR data for **A2** matched well with the expected structure of the gelator molecule. NMR for the gelator was taken in DMSO-d<sub>6</sub>.  $^{1}$ H NMR of **A2** (500 MHz,298K, DMSO-d<sub>6</sub>):  $\delta$  9.7(s,3H), 8.48 (s, 6H), 8.13 (s, 3H).  $^{13}$ C NMR of **A2** (125 MHz, 298K, DMSO-d<sub>6</sub>):  $\delta$  167.12, 164.70, 140.43, 131.98, 125.76, 124.41.

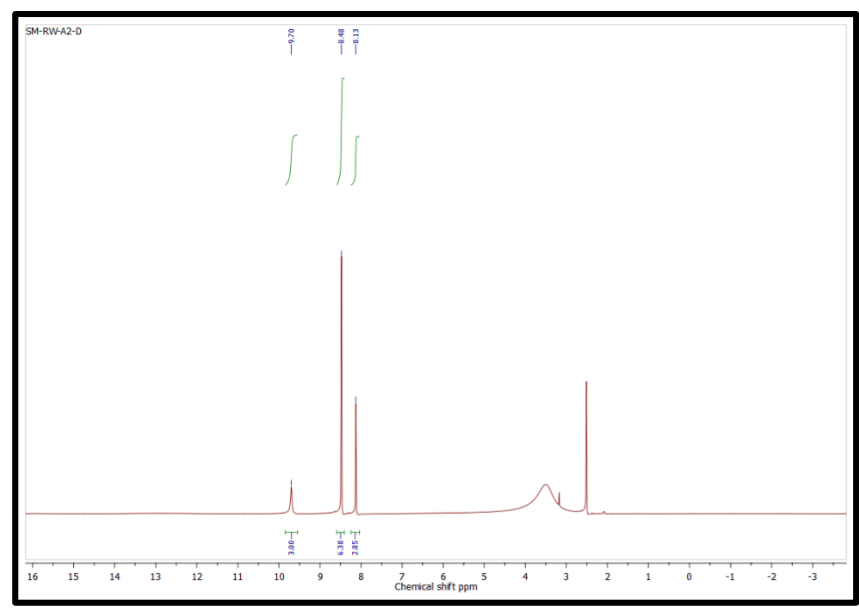


Figure 4.1a: <sup>1</sup>H NMR spectrum of A2

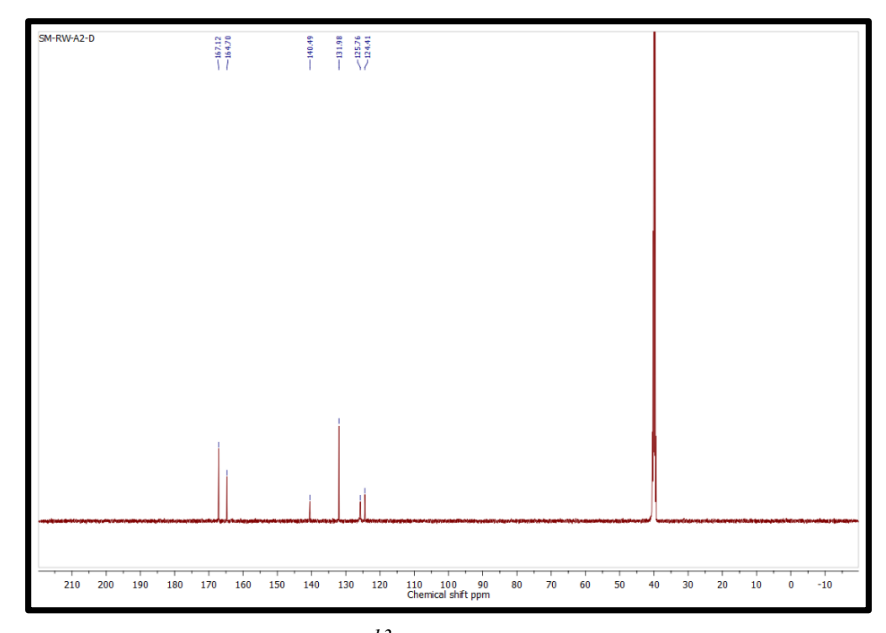


Figure 4.1b: <sup>13</sup>C NMR spectrum of A2

NMR data of the **C1** drug matched with the reported data.  $^{1}$ H NMR (400.13 MHz, 298 K, DMSO-d<sub>6</sub>)  $\delta$ , ppm: 13.29 [s, 1H, H of N-H], 7.69-6.95 [aromatic protons of the ligand], 5.82-5.77 [aromatic protons of p-cymene ring], 3.84 [s, 3H, CH of OCH<sub>3</sub>], 2.85 [m, 1H, CH(CH<sub>3</sub>)<sub>2</sub>], 2.09 [s, 3H, CH of C<sub>6</sub>H<sub>4</sub>CH<sub>3</sub>], 1.20 [d, 6H, CH of C(CH<sub>3</sub>)<sub>2</sub>].

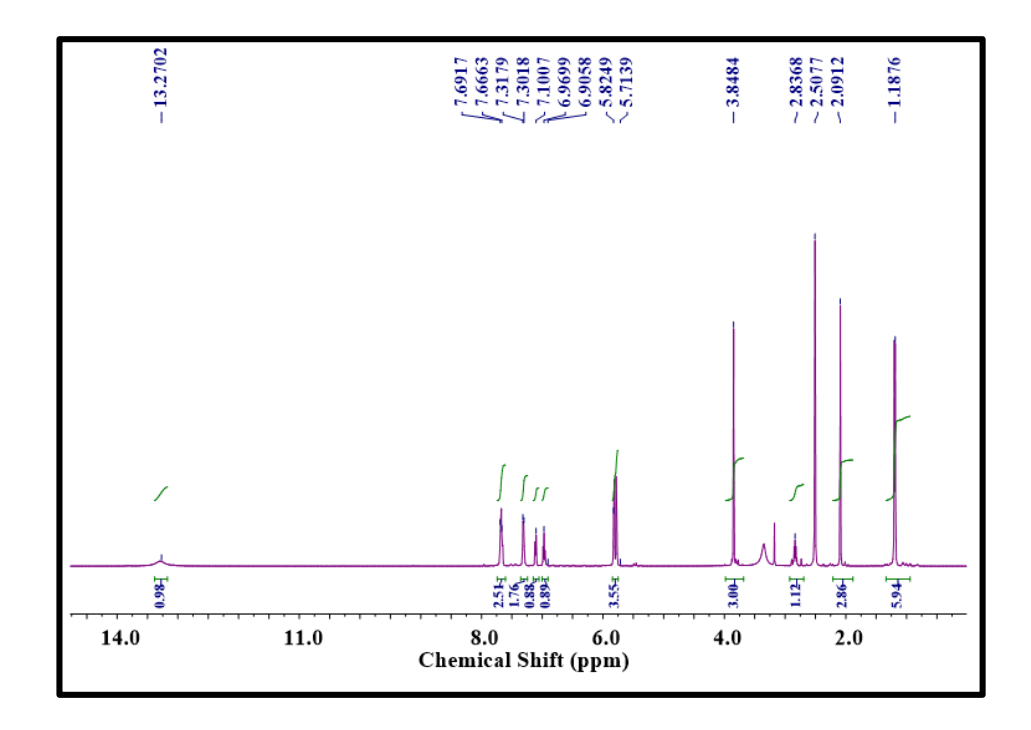


Figure 4.2: <sup>1</sup>H NMR spectrum of C1

## 4.4 Solubility of A2 and Gelation Behavior

The A2 LMWG was found to be soluble in DMSO and DMF, as shown in the table below. The organogel was fabricated by dissolving 15 mg of A2 in 0.65 mL of DMSO, followed by the addition of 0.35 mL of H<sub>2</sub>O. The critical gel concentration of A2 was found to be 10 mg in 1 mL of solvent. The test-tube inversion method was used to verify the gel formation. Similarly, the Cu metallogels were prepared in 1 mL of solvent using the metal salts and A2 in 1:1 proportion. The gel-sol conversion temperature determined by heating-cooling method was found to be 80 °C for all organogels and metallogels, indicating the stability of gels at room temperature.

**Table 4.1:** Solubility of Gelator molecule in various solvents

Solvent	Solubility (A2)	Gelation	Solvent	Solubility (A2)	Gelation
CCl <sub>4</sub>	Insoluble	-	Chloroform	Insoluble	-
Methanol	Insoluble	-	DCM	Insoluble	-
THF	Insoluble	-	DMSO	Soluble	Strong Gel
Toluene	Insoluble	-	Ethanol	Insoluble	-
n-Hexane	Insoluble	-	Benzene	Insoluble	-
DMF	Soluble	Weak Gel	Ethyl Acetate	Insoluble	-
Acetone	Insoluble	-	1,4-dioxane	Insoluble	-

**Table 4.2:** Optimization Table for gelation with fixed gelator concentration

Concentration	DMSO(μL)	H <sub>2</sub> O(μL)	Gelation
15 mg	500	500	Weak gel
	400	600	No gel (only gelation)
	600	400	Gel
	650	350	Strong Gel
	700	300	Fragile gel

**Table 4.3:** Optimization Table for gelation with fixed solvent proportion

Concentration	DMSO/H <sub>2</sub> O	Gelation
7.5 mg	0.65 mL/0.35 mL	No Gel
15 mg	0.65 mL/0.35 mL	Strong gel
22.5 mg	0.65 mL/0.35 mL	Strong gel
30 mg	0.65 mL/0.35 mL	Strong gel
37.5 mg	0.65 mL/0.35 mL	Strong gel



Figure 4.3: Inversion test of Cu metallogel and organogel of A2

### 4.5 Rheological Data

Utilizing rheological methods, the viscoelastic properties of the synthesised gels were investigated. It was observed that the storage modulus (G') for the organogel was around 7147 Pa (figure 4.4b) and that G' was consistently greater than the loss modulus (G") indicating successful gelation. Both results (G' and G") in the linear viscoelastic experiment (LVE) diverged from linearity as the strain increased. The deformation range for organogel was up to 0.5% strain (figure 4.4a). The crossover point comes at 12.47% strain, after which the value of loss modulus becomes greater than storage modulus, indicating that the gel collapses at this point. The thixotropic behaviour of the organogel A2 was further confirmed by time oscillation sweep experiment in the strain range of 0.1% - 100%. After one cycle, the storage modulus of the gel decreased to 3983 Pa due to the removal of excess solvent entrapped in the gel (figure 4.6) Similarly, the rheology tests were done for the Cu metallogel and the storage modulus for Cu metallogel was found to be 3276 Pa (figure 4.5)

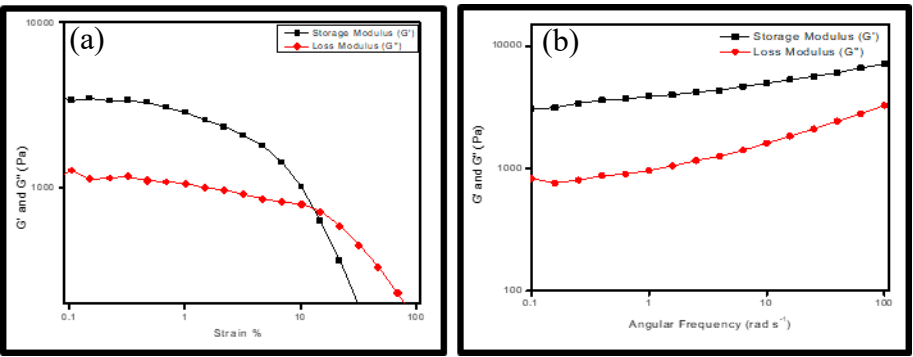


Figure 4.4: (a) Linear viscoelastic behaviour for A2 organogel (b)

Dynamic frequency sweep for the A2 organogel

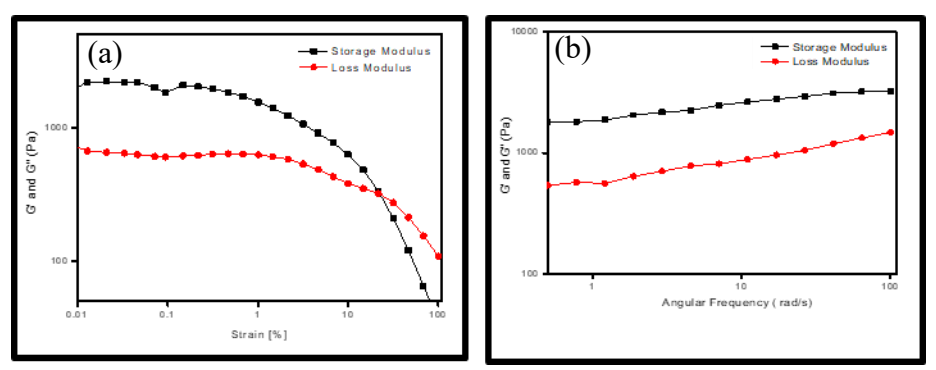


Figure 4.5: (a) Linear viscoelastic behaviour for Cu metallogel (b)

Dynamic frequency sweep for the Cu metallogel

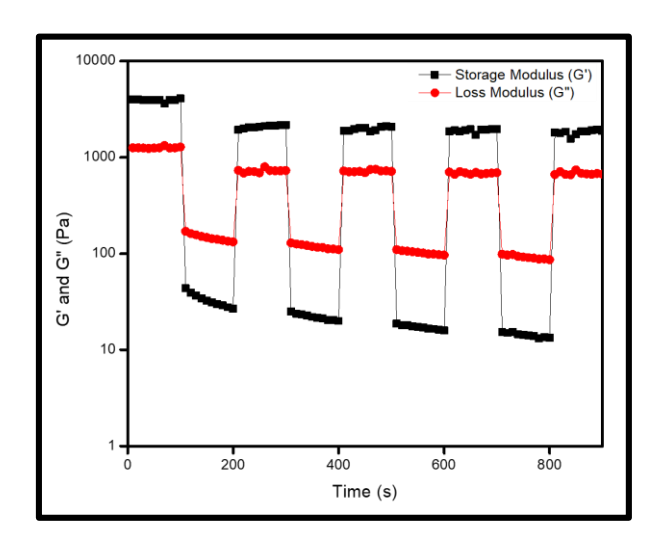


Figure 4.6: Time oscillation sweep (TOS) experiment for A2 organogel

The rheology and viscoelastic behavior of **Ru@A2** gel was also done to confirm the formation and stability of **Ru@A2** gel. The storage modulus for **Ru@A2** was found to be 133 Pa (figure 4.7b). The deformation range of **Ru@A2** was found to be upto 0.5% strain. The crossover point for the **Ru@A2** gel was at 35.92 Pa (figure 4.7a). In frequency sweep experiment, at 0.4 % strain, G' was always greater and parallel to the G," confirming the stability and viscoelastic behavior of gel.

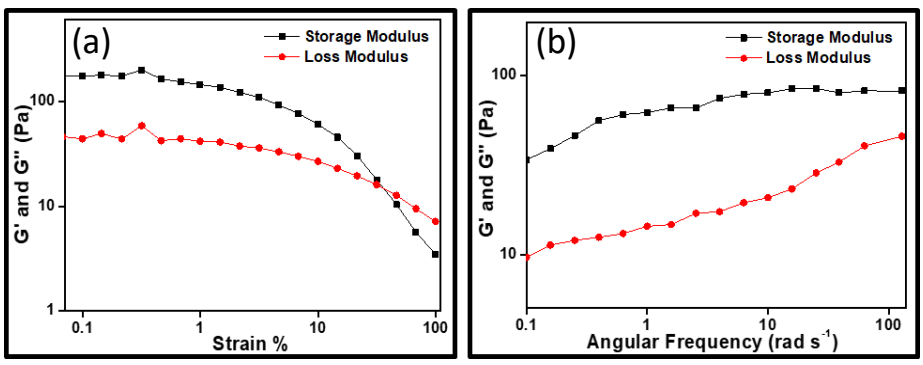


Figure 4.7: (a) Linear viscoelastic behaviour for Ru@A2 metallogel

(b) Dynamic frequency sweep for the Ru@A2 metallogel

## **4.6 FESEM Analysis**

FESEM analysis was conducted to evaluate the morphology of the synthesized gels. FESEM analysis showed that both the organogel and Cu metallogel have nanostructured fibrous morphology. The mapping shows a uniform distribution of elements in the matrices. The presence of different elements was also verified by mapping.

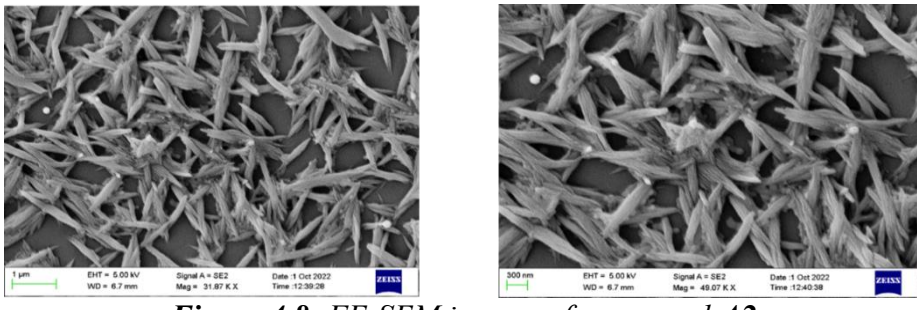


Figure 4.8: FE-SEM images of organogel A2

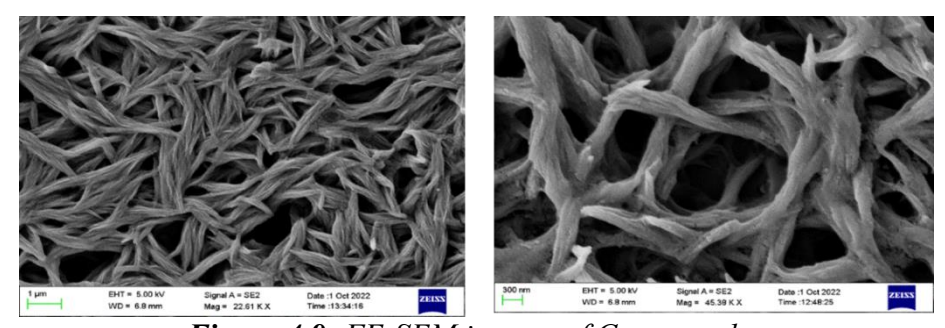


Figure 4.9: FE-SEM images of Cu xerogel

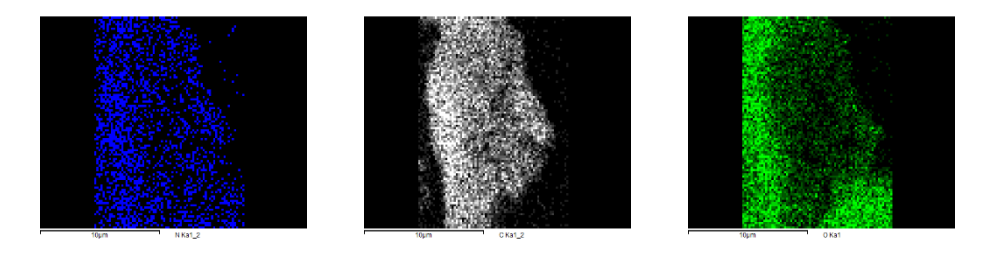


Figure 4.10: Mapping of elements in A2 xerogel

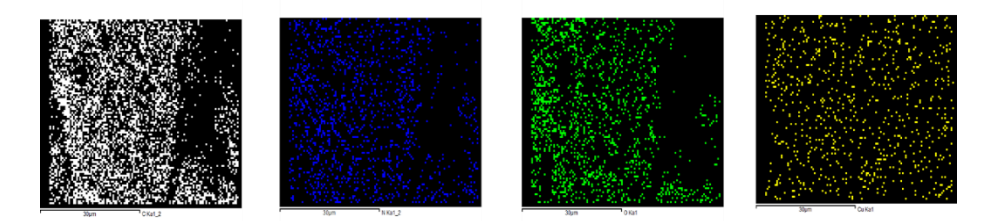


Figure 4.11: Mapping of elements in Cu xerogel

The EDX analysis of organogel shows the presence of C, N, O (figure 4.12) whereas the presence of Cu in the EDX analysis of metallogel along with the other elements (figure 4.13) confirms the successful formation of metallogel.

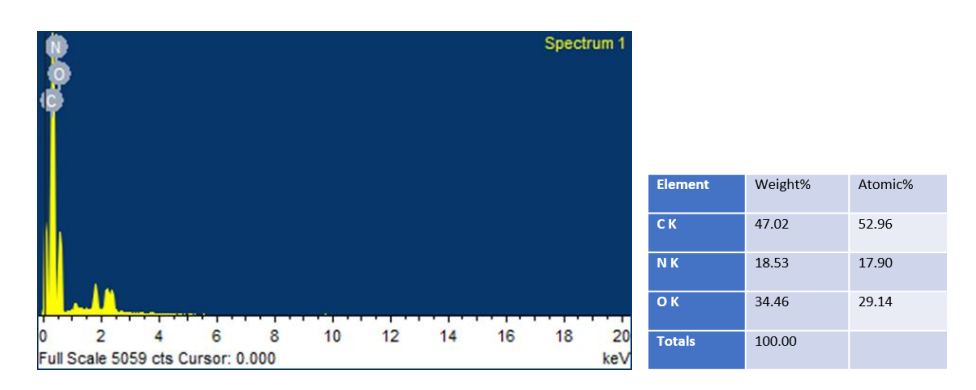


Figure 4.12: EDX analysis of organogel

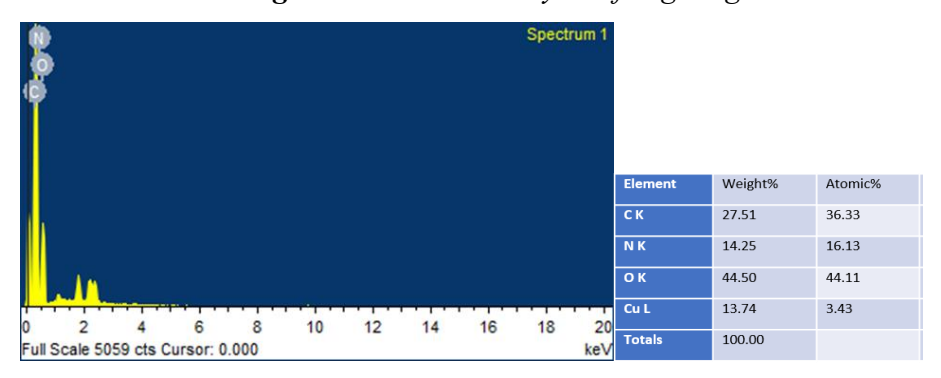


Figure 4.13: EDX analysis of Cu xerogel

## 4.7 Thermogravimetric Analysis

In the temperature range of 25 to 800 °C, the thermogravimetric analysis (TGA) of the xerogels of organogel and Cu metallogel was conducted. The TGA analysis (figure 4.14) showed thermal stability with minimal weight loss up to 150 °C in both the cases. The minimal weight loss up to 150 °C may be due to the removal of entrapped solvent molecules from the compound.

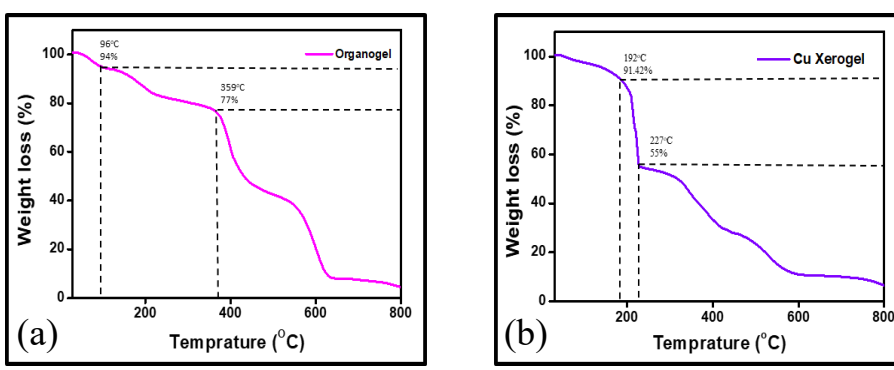


Figure 4.14: TGA analysis of (a) organogel A2, (b) Cu metallogel

#### 4.8 XPS Spectra

The XPS analysis of organogel and copper metallogel was also carried out to confirm the presence of elements. The XPS of organogel (figure 4.15a) confirmed the presence of C, N, H, and O elements. The presence of two peaks in the N1s spectra at around 398.2 and 399.7 eV confirms the presence of C-N and C=N functionalities in the organogel (figure 4.15c). The surface spectra of copper gel confirmed the presence of Cu and Cl in addition to the elements present in **A2** (figure 4.15b). The peaks for C-N and C=N in the copper metallogel shifted to 398.5 eV and 400 eV.

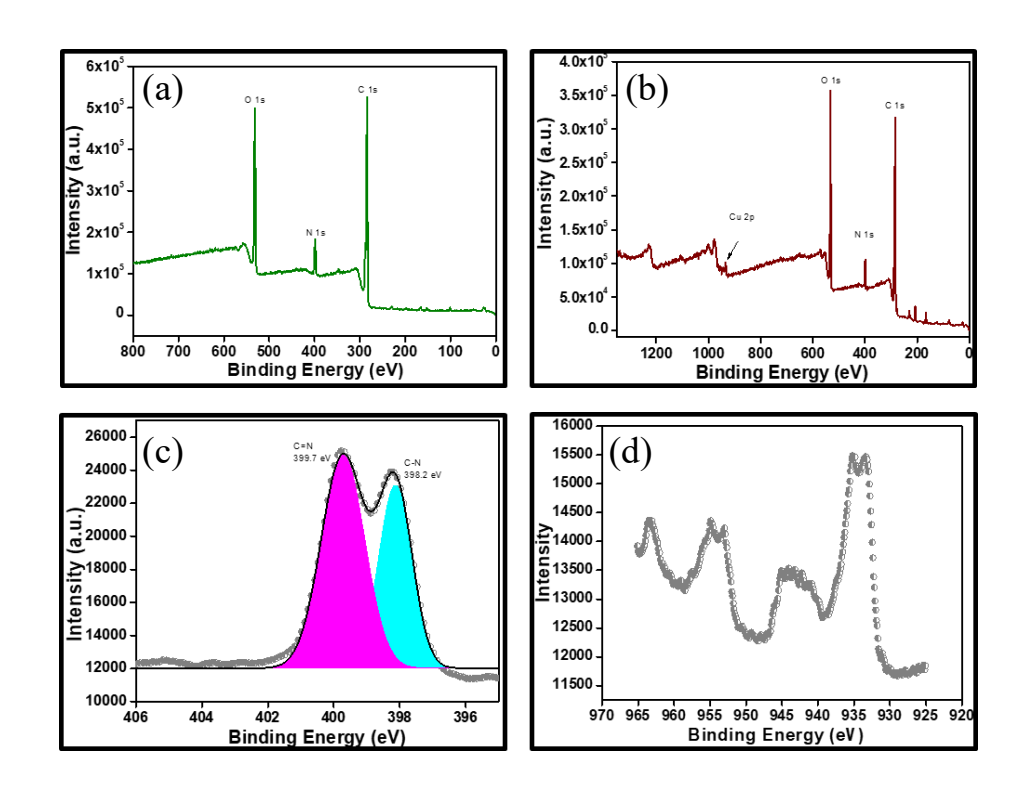


Figure 4.15: XPS surface spectra (a)Nitrogen survey of OG (b) Cu survey of Cu metallogel (c) N1s surface spectra of OG (d) Cu2p surface spectra of Cu metallogel

# 4.9 BET Analysis

The pore size and surface area of organogel and Cu metallogel were calculated from the  $N_2$  adsorption-desorption isotherm at 77 K and 1 bar pressure. The Langmuir surface area for xerogel of organogel was calculated as  $102.997~\text{m}^2\text{g}^{-1}$  and  $72.935~\text{m}^2\text{g}^{-1}$  for Cu metallogel respectively.

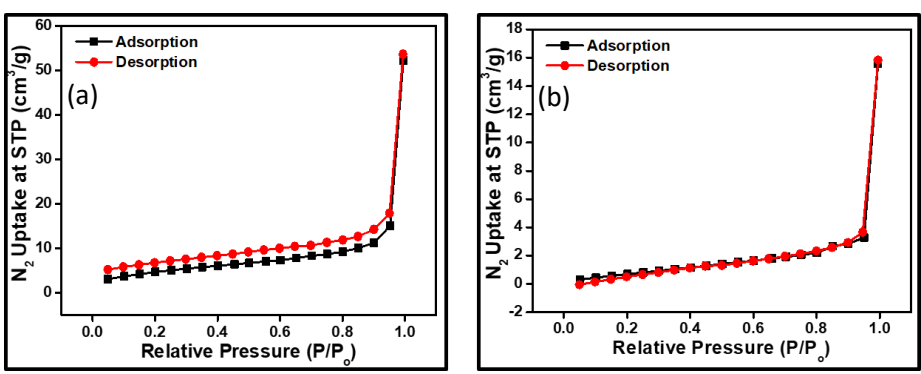


Figure 4.16: N<sub>2</sub> adsorption and desorption isotherm for (a) organogel
(b) Cu metallogel at 77K

The Barrett-Joyner-Halenda (BJH) method was used to plot the pore size distribution which confirmed the mesoporous nature of both the organogel as well as the Cu metallogel. The pore size was found to be 4.11 nm (figure 4.17a) and of 3.07 nm (figure 4.17b) for the organogel and Cu metallogel respectively.

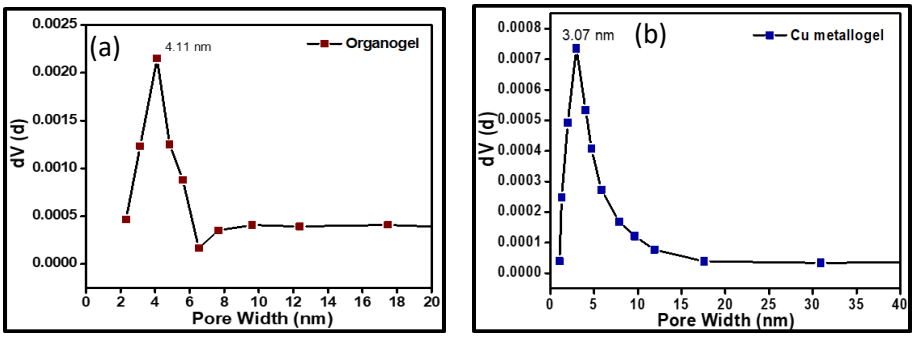
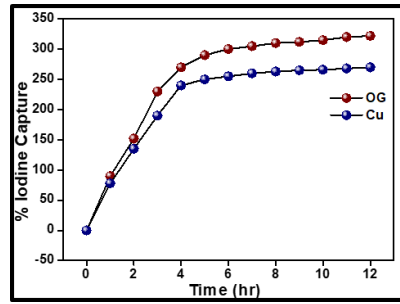


Figure 4.17 BJH pore size distribution for (a) organogel (b) Cu metallogel

### 4.10 Iodine Adsorption in Vapour Phase

Owing to the high surface area and permanent porosity of both organogel and Cu metallogel, iodine uptake ability of the gel materials was investigated. Both the xerogels of organogel and Cu metallogel were exposed to iodine vapour at 75 °C under ambient pressure to mimic the typical nuclear fuel processing condition. Rapid change in color of both the xerogels from their original color to deep brown indicated the adsorption of iodine in the gel matrix. The adsorption capacity of the organogel was found to be 3200 mgg<sup>-1</sup> (320 wt%) whereas the adsorption capacity for Cu metallogel was found to be 2500 mgg<sup>-1</sup> (250 wt%).



**Figure 4.18**: Adsorption of vapour iodine by organogel and Cu metallogel

The adsorption of iodine by organogel and Cu metallogel was confirmed by TGA, XPS, and FESEM analysis. TGA of iodine-adsorbed organogel and Cu metallogel showed an immediate weight loss of up to 100 °C due to the removal of iodine from the gel matrix. The XPS surface spectra of iodine-adsorbed organogel and Cu metallogel confirmed the presence of iodine in the gel matrix.

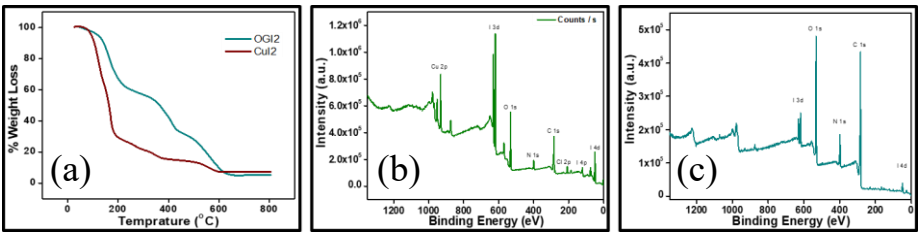


Figure 4.19: (a) TGA analysis of I<sub>2</sub>@OG and I<sub>2</sub>@Cu (b) XPS spectra of I<sub>2</sub>@Cu (c) XPS spectra of I<sub>2</sub>@OG

The FESEM analysis of both the gel showed a change in the fibrous nature. The fibers of the gel matrix got aggregated due to capture of iodine in the pores of the gel matrix.

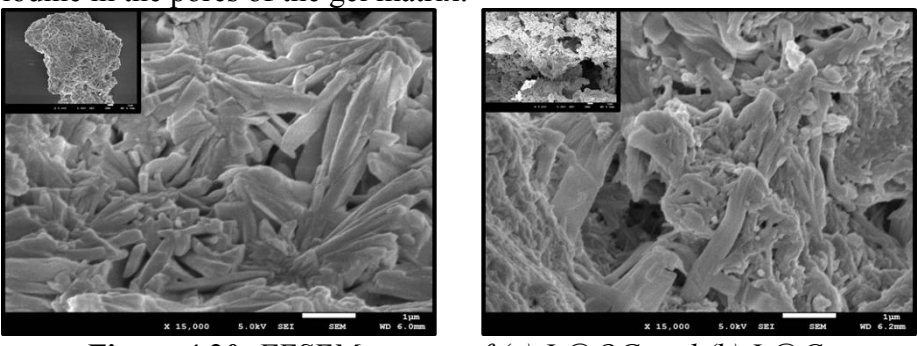


Figure 4.20: FESEM images of (a) I<sub>2</sub>@OG and (b) I<sub>2</sub>@Cu

#### 4.11 Iodine Adsorption by Organogel and Cu Metallogel

Both the organogel and Cu metallogel shows efficient capture of iodine in the gel state from hexane solution. The organogel and Cu metallogel were taken in separate vials and layered with 1 mM hexane solution. Slow disappearance of pink coloration of iodine indicated iodine adsorption. The adsorption of iodine was analyzed by UV-Vis spectroscopy. Both the gels show an iodine adsorption efficiency of more than 97% in ten minutes.

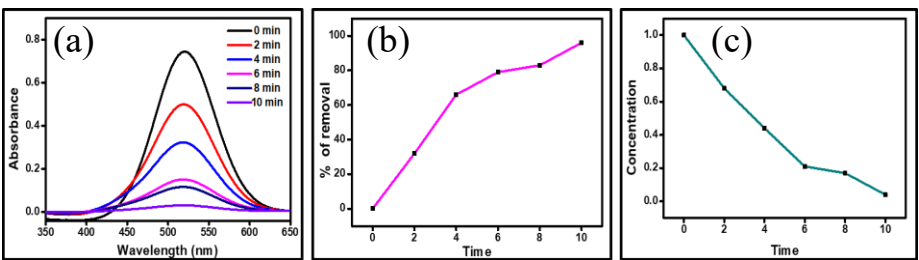


Figure 4.21: (a) Time dependent iodine adsorption by organogel (b) % removal of iodine with time (c) concentration of iodine left (time dependent)

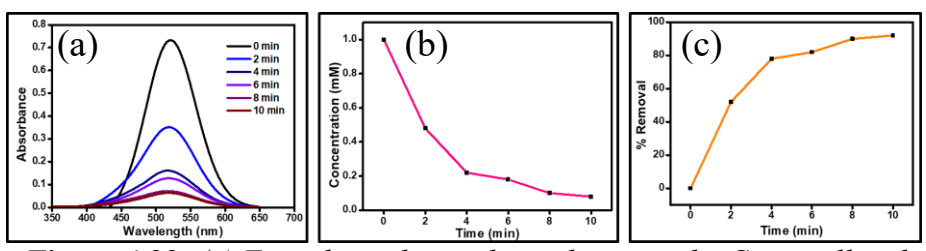


Figure 4.22: (a) Time dependent iodine adsorption by Cu metallogel (b) % removal of iodine with time (c) concentration of iodine left (time dependent)

The adsorption of iodine by gel was found to be following pseudo-second order kinetics as confirmed by the straight-line plot of t/qt vs t having an R<sup>2</sup> value of 0.958 for organogel and 0.97 for copper gel.

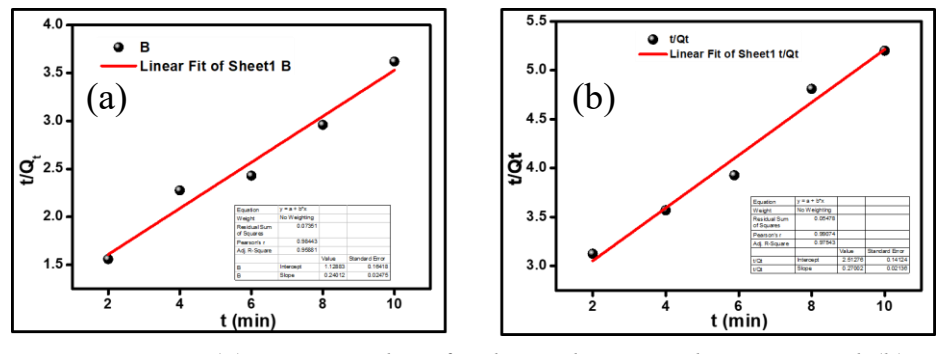


Figure 4.23: (a) Kinetics plot of iodine adsorption by organogel (b)

Kinetics plot of iodine adsorption by Cu metallogel

To determine the adsorption capacity of both the gels, non-linear Langmuir adsorption curve was plotted. The adsorption capacity  $(q_e)$  at equilibrium was calculated at varying concentrations of iodine solutions, and then  $q_e$  value was plotted versus concentration of iodine left after adsorption. The adsorption capacity was found to be 2.5 mgmL<sup>-1</sup> and 1.71 mgmL<sup>-1</sup> for the organogel and Cu metallogel, respectively.

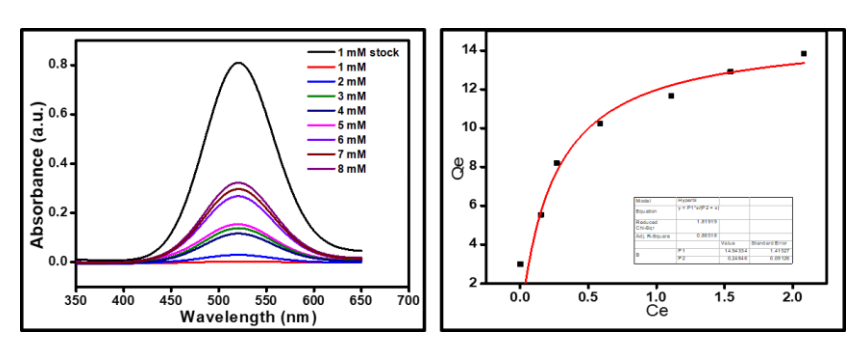


Figure 4.24: Non-linear Langmuir adsorption isotherm for organogel

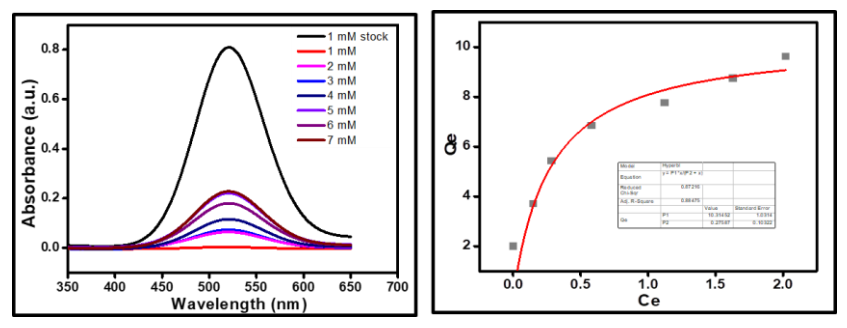


Figure 4.25: Non-linear Langmuir adsorption isotherm for Cu metallogel

After the adsorption, the release of iodine from the adsorbed gel was done by layering the gel with ethanol. Iodine starts getting released from the gel matrix. The same organogel and Cu metallogel was found to be reusable up to five cycles.

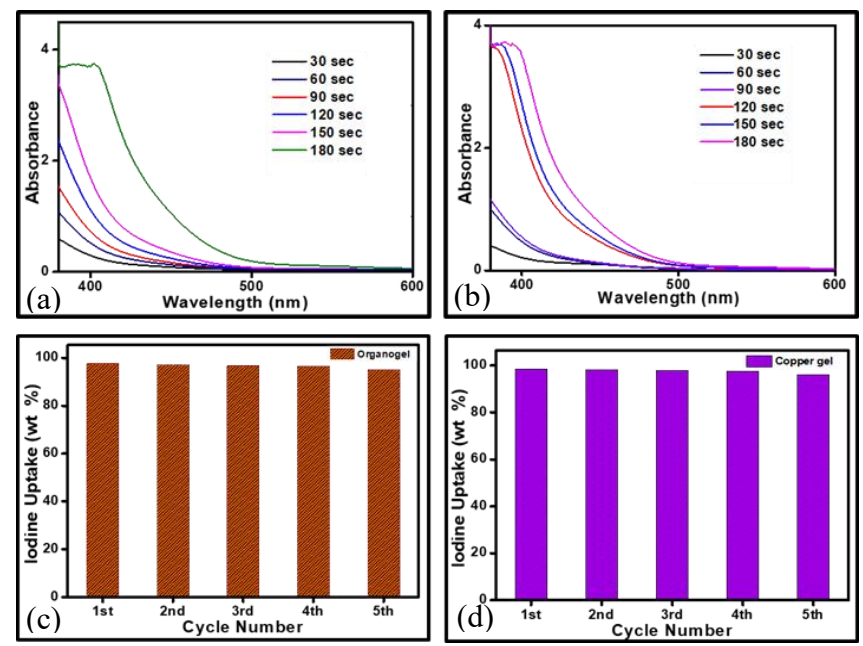
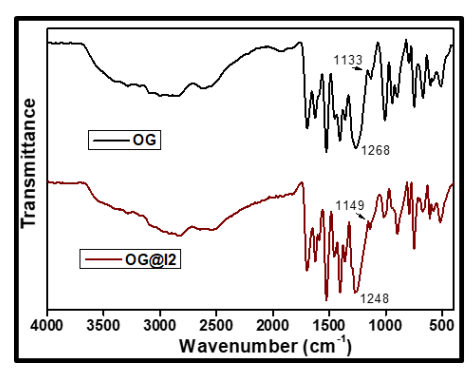


Figure 4.26: (a) UV-vis of iodine release from organogel (b) (a) UV-vis of iodine release from Cu metallogel (c)Reusability of organogel for iodine capture (d) Reusability of Cu metallogel for iodine capture

The possible mechanism for the interaction and adsorption of iodine in the gel matrix is due to the presence of electron withdrawing triazine ring and C-N bond in the **A2** gelator. This triazine ring and C-N group both interacts with the electron rich iodine (I<sub>3</sub>-) ion due to which the iodine gets adsorbed in the gel matrix. These interactions were analyzed by the shift in IR band of triazine C-N group from 1280 to 1270 cm<sup>-1</sup> and 1406 to 1386 cm<sup>-1</sup> in Cu metallogel after iodine adsorption. Similarly, in organogel the band shifted from 1268 to 1248 cm<sup>-1</sup> indicating the interaction of the triazine ring with iodide ion.



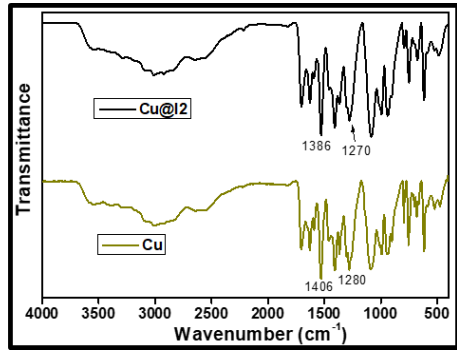


Figure 4.27: (a) Comparison of IR spectra of Cu metallogel and iodine adsorbed Cu metallogel (b) Comparison of IR spectra of organogel and iodine adsorbed organogel

The change in XPS spectra of N1s was also observed for both the C-N and C=N bond. In the organogel C-N and C=N peak shifts from 398.2 eV to 398.37 eV and 399.7 eV to 399.89 eV, respectively indicating the interaction during iodine adsorption. In case of Cu metallogel also, similar shift was observed after iodine adsorption. The C-N and C=N peak shifted from 398.5 eV to 398.61 eV and 400 eV to 400.22 eV respectively.

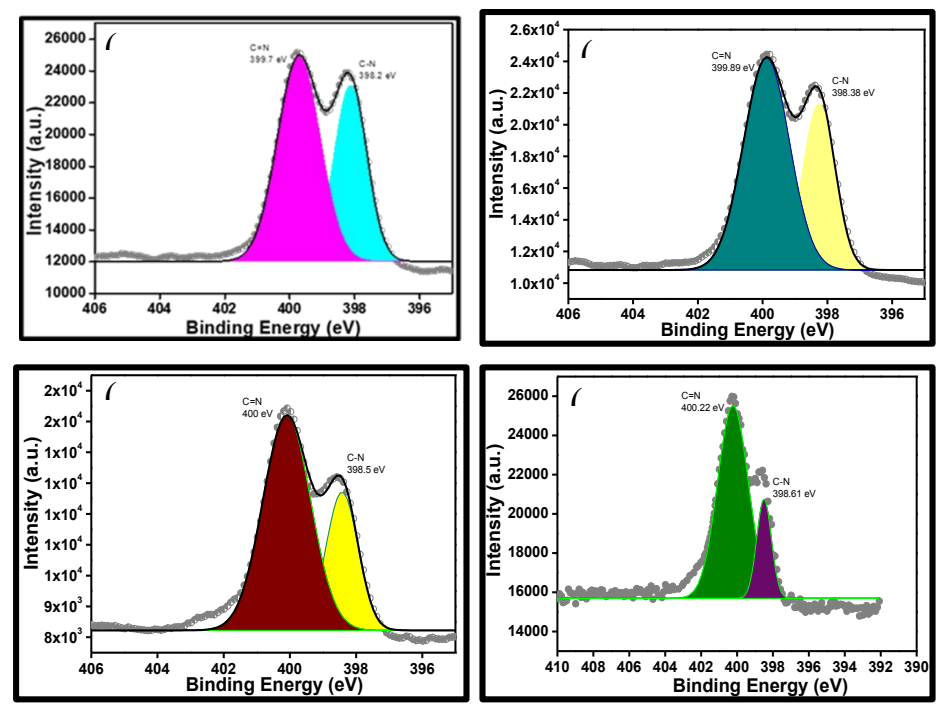
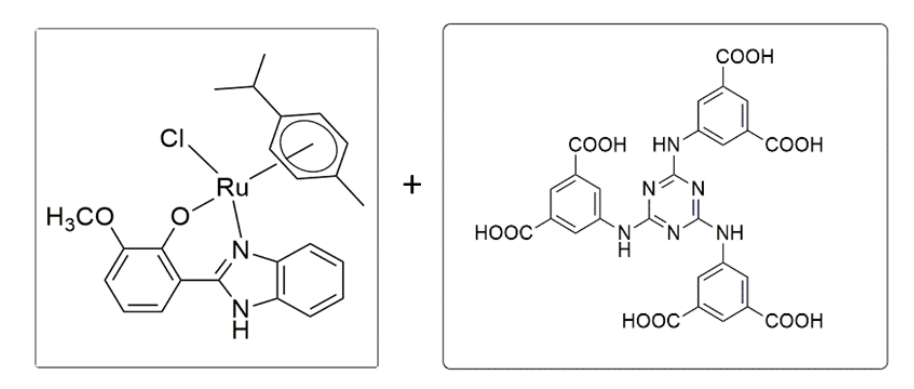


Figure 4.28: (a) N1s XPS spectra of OG (b) N1s XPS spectra of I2@OG (c) N1s XPS spectra of Cu metallogel (d) N1s XPS spectra of I2@Cu

### **4.12 Targeted Drug Delivery**

Inspired by the capability of the oragnogel in trapping foreign molecules, the capability of the gel matrix towards capturing metal based drug molecule was further investigated. In this regard Ru-based drug<sup>47</sup> C1 was loaded in the gel matrix. The gel was formed due to the H-bonding interaction among the carboxylic groups present in the gelator moiety and the C1 drug molecule was simply entrapped in the gel matrix. As the organogel was responsive towards pH, the pH responsive nature of Ru@A2 was also checked. It was observed that the disruption rate of Ru@A2 was rapid in lower pH compared to the neutral pH. Inspired from this observation, the ability of Ru@A2 to deliver the entrapped drug molecule C1 in cancer cells was investigated as the pH of cancer cells are nearly 5.6 due to the presence of lactic acid.



Scheme 4.3: Ru-based anticancer drug loading on A2

#### 4.12.1 **Drug Loading**

The loading of C1 drug was done by simply dissolving drug and A2 gelator in 1:1 equivalent in DMSO. Addition of water in the solution leads to the fabrication of  $\mathbf{Ru@A2}$  gel. To confirm the stability of gel, rheology was done, which showed that, the storage modulus was 83 Pa and always more than loss modulus at 0.4% strain. The loading of drug was confirmed by UV-Vis, IR spectroscopy, TGA, PXRD, and FESEM analysis. The UV-Vis spectra of  $\mathbf{Ru@A2}$  showed similar peaks as of C1 drug at 252 nm, 287 nm, 371 nm corresponding to  $\pi$ - $\pi$ \*, n- $\pi$ \* and MLCT transitions respectively. The IR spectra of  $\mathbf{Ru@A2}$  showed stretching band corresponding to C1.

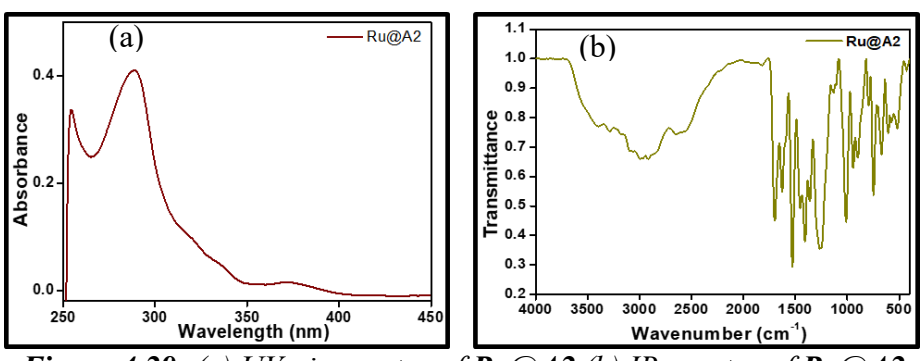


Figure 4.29: (a) UV-vis spectra of Ru@A2 (b) IR spectra of Ru@A2

The TGA of **Ru@A2** showed a sudden loss in weight at nearly 330 °C due to the loss of **C1** drug from the gel matrix. PXRD spectra of **Ru@A2** showed extra peaks as compared to organogel at 2θ value of 45° and 55°

confirming the presence of Ru in the gel matrix. The FESEM of Ru@A2 showed needle-like fibrous morphology.

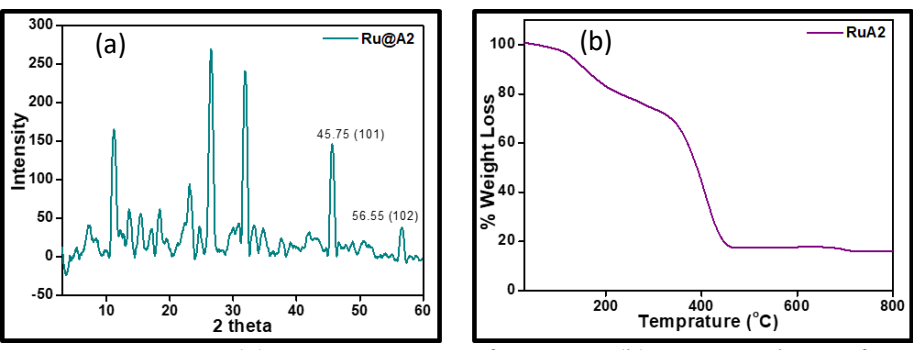


Figure 4.30: (a) PXRD spectra of Ru@A2 (b) TGA analysis of

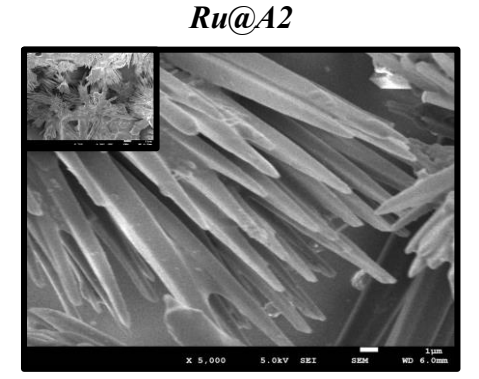


Figure 4.31: FESEM image of Ru@A2

#### 4.12.2 Drug Release

The release of drug from **Ru@A2** gel was analyzed at pH 5.35 and 7.35 of PBS buffer. Layering the **Ru@A2** gel with PBS buffer at pH 5.35 leads to slow release of Ru drug from the gel matrix, observed by the change of layer color from transparent to brown. The solid part became off-white in color. The release of drug **C1** was confirmed by mass spectrometry and NMR spectroscopy. Mass data of released drug gave the most significant peak at 475 m/z corresponding to the **C1** drug itself. NMR data of the released compound matched well with the **C1** drug confirming the release of drug from the gel matrix. <sup>1</sup>H NMR (500 MHz, 298 K, DMSO d6) δ, ppm: 13.29 [s, 1H, H of N-H], 7.69-6.95 [aromatic protons of the ligand], 5.82-5.77 [aromatic protons of p-cymene ring],

3.84 [s, 3H, CH of OCH<sub>3</sub>], 2.85 [m, 1H, CH(CH<sub>3</sub>)<sub>2</sub>], 2.09 [s, 3H, CH of C<sub>6</sub>H<sub>4</sub>CH<sub>3</sub>], 1.20 [d, 6H, CH of C(CH<sub>3</sub>)<sub>2</sub>]

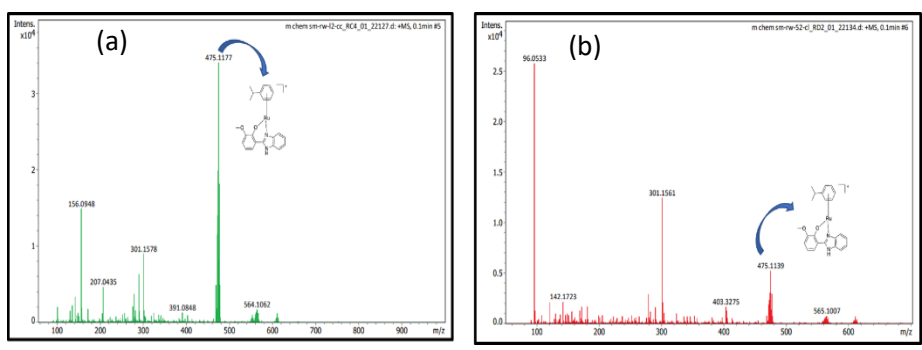


Figure 4.32: (a) ESI-MS spectrum of liquid residue after drug release

(b) ESI-MS spectrum of solid residue after drug release

SM-RW-4QUID

TO SOLID TO SO

Figure 4.33: <sup>1</sup>H NMR spectra of liquid residue after drug release

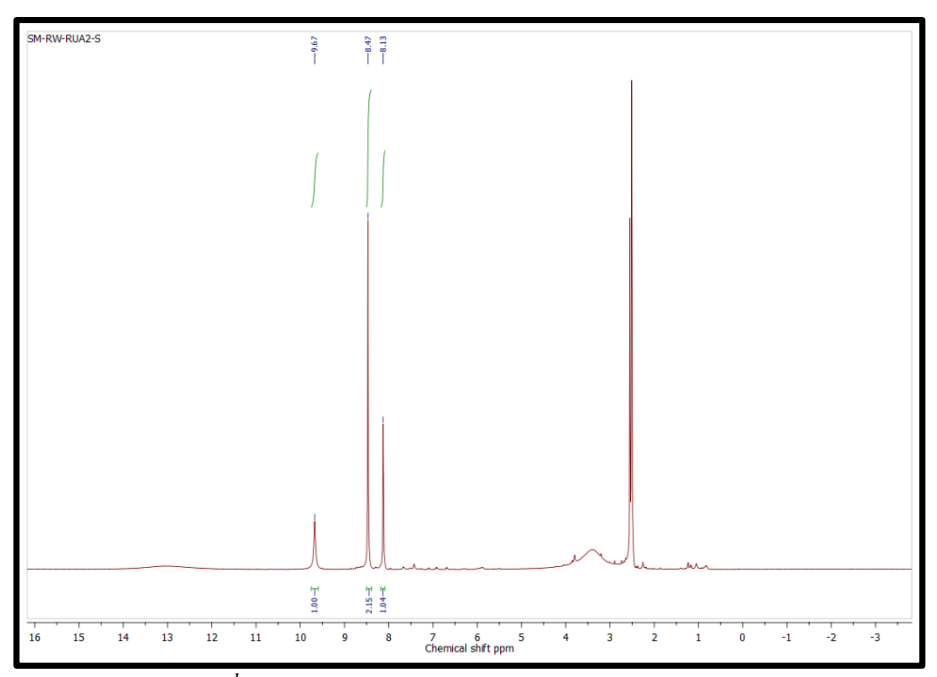


Figure 4.34: <sup>1</sup>H NMR spectra of solid residue after drug release

The time dependent release of drug at acidic pH showed the slow release of drug C1 from gel matrix. The release of drug was calculated and observed using UV-Vis spectroscopy. At pH 5.35, the percentage release of drug after forty-eight hours was around 79%, whereas percentage release of drug was only around 44% at pH 7.35. The enhancement in the release of drug was due to H-bonding disruption in acidic pH.

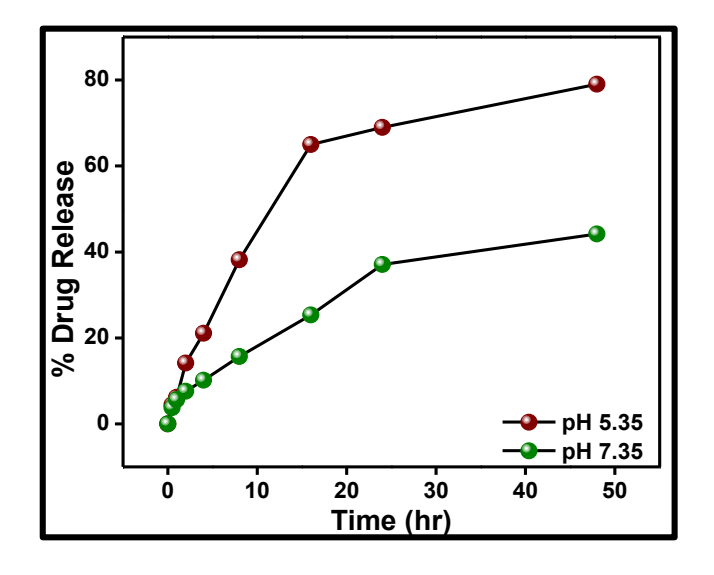


Figure 4.35: Drug release profile of Ru@A2 at different pH

#### **4.12.3 MTT Assay**

Cell viability assays were conducted on cancer cell line HeLa to determine whether the gel can serve as a drug delivery vehicle and whether the loaded drug has anticancer activity. The cancer cells were treated with gelator A2 and drug-loaded gel Ru@A2, and the IC50 value was calculated from a plot of percentage cell viability. The IC50 value clearly shows that the gelator itself is non-cytotoxic, with an IC50 value of 39.94  $\mu$ M. However, when loaded with the ruthenium complex, the gelator demonstrates substantial anticancer activity with a very low IC50 value of 9.689  $\mu$ M. The drug-loaded gelator was also tested for selectivity by treating HEK 293 normal healthy cells with Ru@A2, and the IC50 value was found to be significantly higher, showing the drug's target specificity.

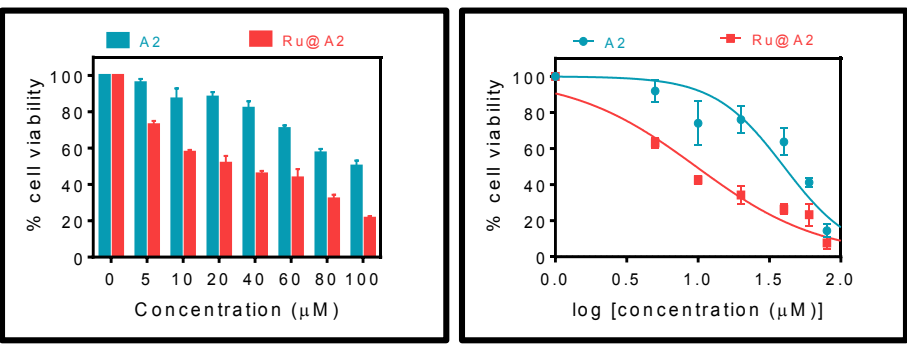


Figure 4.36: MTT Assay of A2 organogel and Ru@A2 gel on HeLa cell

**Table 4.4** IC<sub>50</sub> values for the cytotoxicity of drug on HeLa cancer cells

Compound	HeLa (IC50 values)
A2	$39.94 \pm 0.47$
Ru@A2	$9.689 \pm 0.28$
C1	11.84

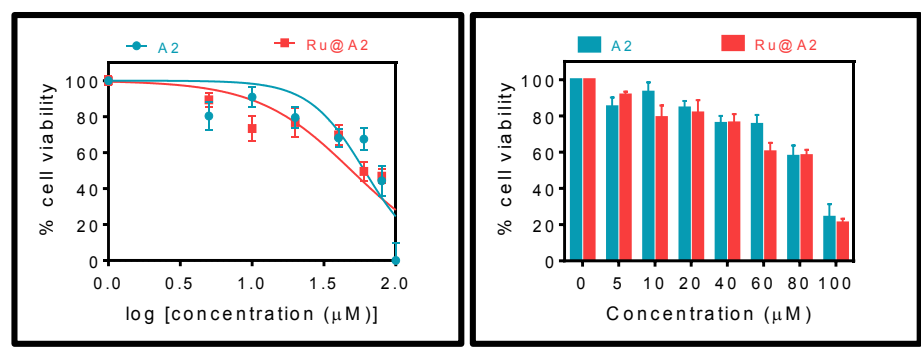


Figure 4.37: MTT Assay of A2 organogel and Ru@A2 gel on HEK
293 cell line

**Table 4.5** IC<sub>50</sub> values for the cytotoxicity of drug on HEK 293 cancer cells

Compound	HEK 293 (IC50 values)
A2	$60.61 \pm 0.69$
Ru@A2	$49.25 \pm 0.53$
C1	39

The activity of drug C1 increased after loading it on A2 gel system which is evident from its IC<sub>50</sub> value. The free drug C1 has an IC<sub>50</sub> value of 11.78  $\mu$ M which decreases to 9.689  $\mu$ M after loading on the gel A2.

## **CHAPTER 5**

# **Conclusion & Future Scope**

#### **5.1 Conclusion**

Design and fabrication of soft materials using low molecular weight gelator (LMWG) molecule opened the way of addressing various intriguing applications in our daily life. The self-assembly resulted due to the noncovalent interactions that were underlying due to the presence of different functionality in LMWG, such as  $\pi$ - $\pi$  stacking, hydrophobic interactions, van der Waals forces, etc. In this work, a gelator molecule A2 is synthesized and characterized using NMR spectroscopy, which under appropriate conditions leads to the fabrication of organogel and metallogel with Cu. The gel fabrication was verified by the test-tube inversion method. The thixotropic behavior of organogel was confirmed by the time oscillation sweep. The FESEM imaging revealed the fibrous morphology of the gels. TGA analysis of organogel, and Cu metallogel has confirmed the stability of the xerogels till 350 °C. The organogel and Cu metallogel further showed the adsorption of iodine in the gel matrices from hexane solution and vapor phase. The iodine adsorption followed a pseudo second order kinetics. Further, the A2 organogel was used to deliver Ru based anticancer drug in cancer cells. Drug delivery was selective in acidic pH with 79% release at 5.35 pH. The IC<sub>50</sub> value for **Ru@A2** on HeLa cancer cells were found to be 9.689 μM.

## **5.2 Future Scope**

The synthesized organogel and Cu metallogel was found to adsorb iodine in their gel matrix, thus it is planned to use these gel matrixes with iodine adsorbed as the antibiotic gel, as it is known that iodine shows antibiotic activity. A thorough investigation of antibiotic activity of organogel and Cu metallogel with iodine adsorption and their mechanistic activity will be done.

### **References**

- Yi T., Sada K., Sugiyasu K., Hatano T., Shinkai S. (2003), Photo-Induced Colour Generation and Colour Erasing Switched by the Sol–Gel Phase Transition, Chem. Commun., 3, 344–345.
   (DOI:10.1039/B210741D)
- (2) Shi C., Huang Z., Kilic S., Xu J., Enick R. M., Beckman E. J., Carr A. J., Melendez R. E., Hamilton A. D. (1999), The Gelation of CO<sub>2</sub>: A Sustainable Route to the Creation of Microcellular Materials, Science, 286 (5444), 1540–1543. (DOI:10.1126/science.286.5444.1540)
- (3) Wang R., Geiger C., Chen L., Swanson B., Whitten D. G. (2000), Direct Observation of Sol–Gel Conversion: The Role of the Solvent in Organogel Formation, J. Am. Chem. Soc., 122 (10), 2399–2400. (DOI:10.1021/ja993991t)
- (4) Malviya N., Sonkar C., Ganguly R., Bhattacherjee D., Bhabak K. P., Mukhopadhyay, S. (2019), Novel Approach to Generate a Self-Deliverable Ru(II)-Based Anticancer Agent in the Self-Reacting Confined Gel Space, ACS Appl. Mater. Interfaces, 11 (50), 47606–47618. (DOI:10.1021/acsami.9b17075)
- (5) Lin Q, Lu T.-T., Zhu X., Sun B., Yang Q.-P., Wei T.-B., Zhang Y.-M. (2015), A Novel Supramolecular Metallogel-Based High-Resolution Anion Sensor Array, Chem. Commun., 51 (9), 1635– 1638. (DOI:10.1039/C4CC07814D)
- (6) Tu T., Fang W., Bao X., Li X., Dötz K. H. (2011), Visual Chiral Recognition through Enantioselective Metallogel Collapsing: Synthesis, Characterization, and Application of Platinum–Steroid Low-Molecular-Mass Gelators, Angew. Chem. Int. Ed., 50 (29), 6601–6605. (DOI:10.1002/anie.201100620)
- (7) Liao Y., He L., Huang J., Zhang J., Zhuang L., Shen H., Su C.-Y. (2010), Magnetite Nanoparticle-Supported Coordination Polymer Nanofibers: Synthesis and Catalytic Application in Suzuki-Miyaura Coupling, ACS Appl. Mater. Interfaces, 2 (8), 2333–2338. (DOI:10.1021/am100354b)

- (8) Lee H., Jung S. H., Han W. S., Moon J. H., Kang S., Lee J. Y., Jung J. H., Shinkai S. (2011), A Chromo-Fluorogenic Tetrazole-Based CoBr<sub>2</sub> Coordination Polymer Gel as a Highly Sensitive and Selective Chemosensor for Volatile Gases Containing Chloride, Chem. Weinh. Bergstr. Ger., 17 (10), 2823–2827. (DOI:10.1002/chem.201003279)
- (9) Mukhopadhyay P., Iwashita Y., Shirakawa M., Kawano S., Fujita N., Shinkai S. (2006), Spontaneous Colorimetric Sensing of the Positional Isomers of Dihydroxynaphthalene in a 1D Organogel Matrix, Angew. Chem. Int. Ed., 45 (10), 1592–1595. (DOI:10.1002/anie.200503158)
- (10) Paul M., Adarsh N. N., Dastidar P. (2012), Cu<sup>II</sup> Coordination
   Polymers Capable of Gelation and Selective SO<sub>4</sub><sup>-2</sup> Separation,
   Cryst. Growth Des., 12 (8), 4135–4143.

   (DOI:10.1021/cg300649e)
- (11) Kar T., Debnath S., Das D., Shome A., Das P. (2009), Organogelation and Hydrogelation of Low-Molecular-Weight Amphiphilic Dipeptides: pH Responsiveness in Phase-Selective Gelation and Dye Removal, Langmuir, 25 (15), 8639–8648. (DOI:10.1021/la804235e)
- (12) Samanta S. K., Bhattacharya S. (2012), Wide-Range Light-Harvesting Donor-Acceptor Assemblies through Specific Intergelator Interactions via Self-Assembly, Chem. Weinh. Bergstr. Ger., 18 (49), 15875–15885. (DOI:10.1002/chem.201103855)
- (13) Draper E. R., Adams D. J. (2017), Low-Molecular-Weight Gels: The State of the Art, Chem, 3 (3), 390–410.(DOI:10.1016/j.chempr.2017.07.012)
- (14) Fang W., Zhang Y., Wu J., Liu C., Zhu H., Tu T. (2018), Recent Advances in Supramolecular Gels and Catalysis, Asian J. Chem., 13 (7), 712–729. (DOI:10.1002/asia.201800017)
- (15) Chen S., Li X., Yu X. (2021), Alkali Metal Ion Triggered
  Conductive and Stimuli-Responsive Metallogels, Dyes Pigments,
  184, 108863-108871. (DOI:10.1016/j.dyepig.2020.108863)

- (16) Pandey V. K., Dixit M. K., Manneville S., Bucher C., Dubey M. (2017), A Multi-Stimuli Responsive Conductive Sonometallogel: A Mechanistic Insight into the Role of Ultrasound in Gelation, J. Mater. Chem. A, 5 (13), 6211–6218. (DOI:10.1039/C7TA00854F)
- (17) Segarra-Maset M. D., Nebot V. J., Miravet J. F., Escuder B.
  (2013), Control of Molecular Gelation by Chemical Stimuli,
  Chem. Soc. Rev., 42 (17), 7086–7098.
  (DOI:10.1039/C2CS35436E)
- (18) Sangeetha N. M., Maitra U. (2005), Supramolecular Gels: Functions and Uses, Chem. Soc. Rev. 2005, 34 (10), 821–836. (DOI:10.1039/B417081B)
- (19) Wen X., Tang L., Li B. (2014), Metallogel Template Fabrication of pH-Responsive Copolymer Nanowires Loaded with Silver Nanoparticles and Their Photocatalytic Degradation of Methylene Blue, Chem.– Asian J., 9 (10), 2975–2983. (DOI:10.1002/asia.201402575)
- (20) Polo-Luque M. L., Simonet B. M., Valcárcel M. (2013), Simple and Fast Fluorimetric Determination of the Critical Gel Concentration of Soft Nanomaterials, Anal. Chim. Acta, 785, 91– 97. (DOI:10.1016/j.aca.2013.04.047)
- (21) Mitchell J. R. (1976) Rheology of Gels, J. Texture Stud., 7 (3), 313–339. (DOI:10.1111/j.1745-4603.1976.tb01140.x)
- (22) Hong Y., Lam J. W. Y., Tang B. Z. (2009), Aggregation-Induced Emission: Phenomenon, Mechanism and Applications, Chem. Commun., 29, 4332–4353. (DOI:10.1039/B904665H)
- (23) Castilla A. M., Dietrich B., Adams D. J. (2018), Using Aggregation-Induced Emission to Understand Dipeptide Gels, Gels Basel Switz., 4 (1), 17-24. (DOI:10.3390/gels4010017)
- (24) Mei J., Leung N. L. C.; Kwok R. T. K., Lam J. W. Y., Tang B. Z.
  (2015), Aggregation-Induced Emission: Together We Shine,
  United We Soar!, Chem. Rev., 115 (21), 11718–11940.
  (DOI:10.1021/acs.chemrev.5b00263)

- (25) Radioactive Iodine (Radioiodine) Therapy for Thyroid Cancer. https://www.cancer.org/cancer/thyroidcancer/treating/radioactive-iodine.html (accessed 2023-04-27).
- (26) Huve J., Ryzhikov A., Nouali H., Lalia V., Augé G., Jean Daou T. (2018), Porous Sorbents for the Capture of Radioactive Iodine Compounds: A Review, RSC Adv., 8 (51), 29248–29273. (DOI:10.1039/C8RA04775H)
- (27) Mondal S., Alam N., Sahoo S., Sarma D. (2023), A "Heat Set" Zr-Diimide Based Fibrous Metallogel: Multiresponsive Sensor, Column-Based Dye Separation, and Iodine Sequestration, J. Colloid Interface Sci., 633, 441–452. (DOI:10.1016/j.jcis.2022.11.111)
- (28) Paul S. D., Sharma H., Jeswani G., Jha A. K., (2017), Novel gels: Implications for Drug Delivery, Nanostructures for Drug Delivery, 12, 379-412. (DOI: 10.1016/B978-0-323-46143-6.00012-9)
- (29) Sosnik A., Seremeta K. (2017), Polymeric Hydrogels as
  Technology Platform for Drug Delivery Applications, Gels, 3(3),
  25-46. (DOI:10.3390/gels3030025)
- (30) Li J., Mooney D. J. (2016), Designing Hydrogels for Controlled Drug Delivery, Nat. Rev. Mater., 1 (12), 1–17. (DOI:10.1038/natrevmats.2016.71)
- (31) Alam N., Sarma D. (2020), Tunable Metallogels Based on Bifunctional Ligands: Precursor Metallogels, Spinel Oxides, Dye and CO<sub>2</sub> Adsorption, ACS Omega, 5 (28), 17356–17366. (DOI:10.1021/acsomega.0c01710)
- (32) Kyarikwal R., Kumar Kundu B., Chakraborty A., Mukhopadhyay S. (2022), A Tris-Tetrazole Based Nanostructured Soft Material: Studies on Self-Healing, AIEE, and Rheological and Fluorometric Detection of 3-Aminopyridine, Mater. Chem. Front., 6 (19), 2835–2847. (DOI:10.1039/D2QM00520D)
- (33) Kyarikwal R., Malviya N., Chakraborty A., Mukhopadhyay S.
  (2021), Preparation of Tris-Tetrazole-Based Metallogels and
  Stabilization of Silver Nanoparticles: Studies on Reduction

- Catalysis and Self-Healing Property, ACS Appl. Mater. Interfaces, 13 (49), 59567–59579. (DOI:10.1021/acsami.1c19217)
- (34) Sarkar K., Dastidar P. (2019), Rational Approach Towards Designing Metallogels From a Urea-Functionalized Pyridyl Dicarboxylate: Anti-Inflammatory, Anticancer, and Drug Delivery, Asian J. Chem., 14 (1), 194–204. (DOI:10.1002/asia.201801462)
- (35) Ghosh A., Das P., Kaushik R., Damodaran K. K., Jose D. A. (2016), Anion Responsive and Morphology Tunable Tripodal Gelators, RSC Adv., 6 (86), 83303–83311. (DOI:10.1039/C6RA16345A)
- (36) Malviya N., Sonkar C., Kundu B. K., Mukhopadhyay S. (2018), Discotic Organic Gelators in Ion Sensing, Metallogel Formation, and Bioinspired Catalysis, Langmuir, 34 (38), 11575–11585. (DOI:10.1021/acs.langmuir.8b02352)
- (37) Malviya N., Sonkar C., Ganguly R., Mukhopadhyay S. (2019), Cobalt Metallogel Interface for Selectively Sensing L-Tryptophan among Essential Amino Acids, Inorg. Chem., 58 (11), 7324– 7334. (DOI:10.1021/acs.inorgchem.9b00455)
- (38) Zhu Y., Qi Y., Guo X., Zhang M., Jia Z., Xia C., Liu N., Bai C., Ma L., Wang Q. (2021), A Crystalline Covalent Organic Framework Embedded with a Crystalline Supramolecular Organic Framework for Efficient Iodine Capture, J. Mater. Chem. A, 9 (31), 16961–16966. (DOI:10.1039/D1TA03879F)
- (39) Alam N., Sarma D. (2020), A Thixotropic Supramolecular Metallogel with a 2D Sheet Morphology: Iodine Sequestration and Column Based Dye Separation, Soft Matter, 16 (47), 10620–10627. (DOI:10.1039/D0SM00959H)
- (40) Marullo S., Tiecco M., Germani R., D'Anna F. (2022), Highly Recyclable Surfactant-Based Supramolecular Eutectogels for Iodine Removal, J. Mol. Liq., 362, 119712-119728. (DOI:10.1016/j.molliq.2022.119712)

- (41) Rambabu D., Negi P., Dhir A., Gupta A., Pooja. (2018), Fe(III) and Cu(I) Based Metal Organic Gels for in Situ Drug Loading and Drug Delivery of 5-Fluorouracil, Inorg. Chem. Commun., 93, 6–9. (DOI:10.1016/j.inoche.2018.04.028)
- (42) Lee J. H., Kim K. Y., Jung J. H. (2019), Self-Assembled Gels Formed by Covalent-Bond That Is Able to Include Drug, Eur. Polym. J., 118, 280–285. (DOI:10.1016/j.eurpolymj.2019.05.055)
- (43) Cheng Y., He C., Ding J., Xiao C., Zhuang X., Chen X. (2013), Thermosensitive Hydrogels Based on Polypeptides for Localized and Sustained Delivery of Anticancer Drugs, Biomaterials, 34 (38), 10338–10347. (DOI:10.1016/j.biomaterials.2013.09.064)
- (44) Zhang B., Dong X., Xiong Y., Zhou Q., Lu S., Liao Y., Yang Y., Wang H. (2020), A Heat-Set Lanthanide Metallogel Capable of Emitting Stable Luminescence under Thermal, Mechanical and Water Stimuli, Dalton Trans., 49 (9), 2827–2832. (DOI:10.1039/C9DT04713A)
- (46) Kolmakov K. A. (2008), An Efficient, "Green" Approach to Aryl Amination of Cyanuric Chloride Using Acetic Acid as Solvent, J. Heterocycl. Chem., 45 (2), 533–539. (DOI:10.1002/jhet.5570450236)
- (47) Porwal P., Nayek S., Singh S., Sonawane A., Grabchev I., Ganguly R., Mukhopadhyay S. (2023), Studies on Anticancer Properties with Varying Co-Ligands in Ru(II) Arene Benzimidazole System, Dalton Trans., Advance Article. (DOI:10.1039/D3DT00528C)